processes

MDPI

Review

Anaerobic Membrane Bioreactor (AnMBR) for the Removal of Dyes from Water and Wastewater: Progress, Challenges, and Future Perspectives

Amin Mojiri [1,2,*], John L. Zhou [3], Bahareh KarimiDermani [4], Elham Razmi [5] and Norhafezah Kasmuri [6]

[1] School of Environmental Science and Engineering, Nanjing University of Information Science and Technology, Nanjing 210044, China
[2] Institute of Textile Research and Industrial Cooperation of Terrassa (INTEXTER), Universitat Politècnica de Catalunya—BarcelonaTech, Colom 15, 08222 Terrassa, Spain
[3] School of Civil and Environmental Engineering, University of Technology Sydney, Sydney 2007, Australia; junliang.zhou@uts.edu.au
[4] Department of Geological Sciences, Hydrogeology, University of Alabama, Tuscaloosa, AL 35487, USA; baharkarimi2828@gmail.com
[5] Department of Environmental Health Engineering, School of Public Health, Iran University of Medical Sciences, Tehran 1449614535, Iran; e_razmi63@yahoo.com
[6] School of Civil Engineering, College of Engineering, Universiti Teknologi MARA (UiTM), Shah Alam 40450, Malaysia; norhafezahkasmuri@uitm.edu.my
* Correspondence: amin.mojiri@gmail.com

Abstract: The presence of dyes in aquatic environments can have harmful effects on aquatic life, including inhibiting photosynthesis, decreasing dissolved oxygen levels, and altering the behavior and reproductive patterns of aquatic organisms. In the initial phase of this review study, our aim was to examine the categories and properties of dyes as well as the impact of their toxicity on aquatic environments. Azo, phthalocyanine, and xanthene are among the most frequently utilized dyes, almost 70–80% of used dyes, in industrial processes and have been identified as some of the most commonly occurring dyes in water bodies. Apart from that, the toxicity effects of dyes on aquatic ecosystems were discussed. Toxicity testing relies heavily on two key measures: the LC50 (half-lethal concentration) and EC50 (half-maximal effective concentration). In a recent study, microalgae exposed to Congo Red displayed a minimum EC50 of 4.8 mg/L, while fish exposed to Disperse Yellow 7 exhibited a minimum LC50 of 0.01 mg/L. Anaerobic membrane bioreactors (AnMBRs) are a promising method for removing dyes from water bodies. In the second stage of the study, the effectiveness of different AnMBRs in removing dyes was evaluated. Hybrid AnMBRs and AnMBRs with innovative designs have shown the capacity to eliminate dyes completely, reaching up to 100%. *Proteobacteria*, *Firmicutes*, and *Bacteroidetes* were found to be the dominant bacterial phyla in AnMBRs applied for dye treatment. However, fouling has been identified as a significant drawback of AnMBRs, and innovative designs and techniques are required to address this issue in the future.

Keywords: biological methods; dyes; AnMBR; wastewater

Citation: Mojiri, A.; Zhou, J.L.; KarimiDermani, B.; Razmi, E.; Kasmuri, N. Anaerobic Membrane Bioreactor (AnMBR) for the Removal of Dyes from Water and Wastewater: Progress, Challenges, and Future Perspectives. *Processes* **2023**, *11*, 855. https://doi.org/10.3390/pr11030855

Academic Editor: Antoine Trzcinski

Received: 16 February 2023
Revised: 9 March 2023
Accepted: 10 March 2023
Published: 13 March 2023

1. Introduction

Access to clean water is crucial for human health and the advancement of society. However, the decline in water quality has become a serious global issue due to human activities [1,2]. The United Nations introduced 17 Sustainable Development Goals (SDGs) with the aim of creating a sustainable future for all humankind. One of the most significant of these goals is "Clean Water and Sanitation for All" [3]. However, the discharge of various contaminants into aquatic environments impedes progress towards achieving SDG6. Among industrial effluents, the textile and dye industries are considered to be major contributors to wastewater production. Dyestuffs, which are synthetic, complex

aromatic compounds, and ionizing agents, are widely used as coloring agents in industries such as paper, textiles, food, dyeing, and cooking [4,5]. Following the dyeing process, approximately 15% of the used dyes remain in the wastewater stream, making the colored wastewater effluent a major concern. Conventional wastewater treatment plants have difficulty in removing such chemicals, resulting in over 200,000 tons of dyes being discharged each year in the environment [6]. The release of dyes results in water pollution with resistant compounds that are not easily broken down by natural degradation processes [7,8].

Several methods have been established for treating dyes from water bodies, including physicochemical and biological approaches [9,10]. Physicochemical methods, such as membrane filtration, adsorption, ion exchange, advanced oxidation processes (AOPs), and coagulation, have limitations in the removal of dyes due to high cost, inefficiency, and the potential for secondary pollution. In contrast, biological treatment methods [11], such as membrane bioreactors (MBRs), are cost-effective, safe, environmentally friendly, and efficient for removing dyes [4]. Among the various biological treatment methods, MBRs are regarded as one of the most effective methods for treating wastewater. MBRs are a combination of units for biological degradation and physical filtration [12]. Castrogiovanni et al. [13] noted that MBRs are effective in treating various emerging contaminants and organic pollutants, including dyes, and also in reducing the emission of greenhouse gases and biological pollutants (such as viruses). Zhang et al. [14] and Deng et al. [15] listed several key advantages of MBRs, including high effluent quality, minimal sludge production, a small footprint, high-quality effluents, and enhanced ability to remove pollutants.

Despite some studies on dye removal by MBRs [16,17], there remains a lack of information about the characteristics of dyes and their removal mechanisms using MBRs. This review paper aims to fill the relevant knowledge gap.

2. Types of Dyes

Effluent from various industrial sectors, such as textile, leather, food processing, and cosmetics, contain synthetic dyes, which can negatively impact aquatic life, ecosystems, and public health [18,19]. The structure of dyes consists of two components: (1) the auxochrome, which affects the water solubility and textile fiber binding, and (2) the chromophore, which determines the color. There are ten classifications of dyes based on their chemical structure: azo, phthalocyanines, xanthene, nitro, quinoline, indigo, acridine, azine, anthraquinone, and triarylmethane [20]. Dyes can also be classified into 14 categories based on their applications, such as vat, insoluble azo, direct, acid, reactive, fluorescent brighteners, fluorescent, basic, and cationic dyes, disperse, polycondensation, oxidation, sulfur, soluble vat, acid mordant, and acid medium dyes [21].

Azo dyes, which make up 50% of dyes used in the textile industry and 60% of all dyestuffs, are known for their persistence in the environment and difficulty in degradation [22,23]. Currently, there are 2000 types of azo dyes in use globally, with an annual production of 70,000 tons. These dyes consist of a combination of diazotized amine and either an amine or a phenol with one or more azo linkages (-N=N-) [24,25]. The classification of azo dyes is based on the number of linkages, such as monoazo (e.g., aniline yellow, reactive orange 16, orange-II, and acid orange-12), diazo (e.g., Congo red, oil red, direct blue-1, reactive black 5, and sudanblack-B), triazo (e.g., direct blue-71), tetraazo (e.g., direct black-22), and polyazo [26]. A comprehensive list of commonly used azo dyes is summarized in Table 1.

Almost 25% of all synthetic dyes belong to the phthalo-cyanine group, according to Tajiki and Abdouss [27]. Phthalocyanine groups are amphiphilic macrocyclic compounds and have a tendency to self-associate due to hydrophobic and π-π electron interactions [28]. Reactive Blue 21 (RB21) is a commonly used organic phthalocyanine in the textile industry [29]. Furthermore, reactive phthalocyanine dyes are frequently utilized in the textile industry to produce blue and green hues, primarily through the use of copper phthalocyanines [30], including Reactive Blue 7 (RB7) [31]. According to Silva et al. [30], reactive phthalocyanines are commonly known for their high water solubility and resistance to

biological degradation and are not effectively removed by adsorption. Table 1 displays the main reported phthalocyanines.

Another widely applied dye group in food, paper, cosmetics, and ink industries is xanthene, which has poor biodegradability because of its superior dyeing and coloring properties [32]. In these dyes, the chromophore includes the planar skeleton of the oxygen-containing heterocyclic compound xanthene [33]. Rhodamine B (RB), phloxine B (PB), basic red 11 and erythrosine B (EB) are widely applied xanthene groups [34], which properties are shown in Table 1. Usually, xanthene dyes display green to red fluorescence (almost 500–600 nm), and thus most fluorescent probes based on these dyes work in the green to red region [35].

Nitro dyes (–NO_2), which range in color from yellow to orange, are a small group of dyes that contain one or more nitro groups (–NO_2) [36]. The N-O and N=O bonds in the nitro group are equal due to resonance and are linked with the resonating C-C and C=C bonds of the aromatic ring. If the substance is a phenol, it exists in a state of balance with a quinonoidone [33]. The nitro group has usually a low color strength ($€_{max}$ = 5000–7000) [36]. Picric acid (CI 10305) and naphthol yellow S (CI 10316), acid orange 3, C.I. disperse yellow 42, and C.I. disperse yellow 70 are the most reported nitro groups [33,36].

Quinolines (quinophthalone) are a type of dye that has garnered significant attention from researchers across multiple fields due to their prevalence in natural products and drugs. Additionally, derivatives of quinolines have applications in polymer chemistry, electronics, and organic optoelectronics. With superior mechanical properties, these compounds are utilized as highly effective electron transport materials (ETMs) [37]. Industrially, quinophthalone dyes are utilized as colorants for plastics and polyester textiles due to their moderate hydrophobicity. These dyes also have applications in biological research, as some exhibit a higher affinity for cell membranes compared to extra- or intracellular fluids [33]. Disodium 2-(2-quinolyl)indan-1,3-dione sulfonate (quinoline yellow) is one of the most widely reported dyes of this group [38].

Indigo is a class of carbonyl compounds and is one of the earliest known natural blue dyes, derived from the Indigofera tinctoria plant. It is being used as a natural food dye to minimize the use of synthetic dyes, which have been linked to carcinogenic effects [39]. In addition, indigo dye is widely utilized by the textile industry and is recognized as a persistent substance, raising environmental concerns [40]. Indigo carmine (IC) is widely applied in industry. The indigo carmine structure is made up of four benzene rings and two sulfonates with a negative charge, resulting in its non-biodegradability, high toxicity, and carcinogenic effects on both humans and aquatic life [18].

The nitrogen heteroatom makes acridine dye weakly basic. Acridine derivatives are important in pharmaceuticals and are used as model compounds in drug-protein/DNA interaction studies. Acridine dye is a useful fluorescence probe in microheterogeneous systems and exists in two forms (neutral and protonated) in aqueous solutions depending on pH [41]. Acridine orange (AO) and acridine yellow G (AY) are two commonly used members of the acridine group [42]. Acridine orange (AO) is a basic fluorescent cationic compound used in the manufacture of ink, leather, and textiles [43].

Azine dyes (=N-N=) are widely used in the textile industry and related industries [44]. Azine dyes contain the phenazine skeleton, a flat aromatic compound made of two linked benzene rings connected by two nitrogen atoms. The chromophore has a spread out positive charge and alternates between aromatic and quinonoid structures [33]. Methylene Blue (MB), thionin (TH), and safranin O (SO) are widely used azine dyes [45].

Anthraquinone can have various substitutions, including connections with other ring systems that are fused together. This group of carbonyl dyes, which comprises hundreds of compounds, is the largest in production and is used in a multitude of ways on textiles [33]. Due to their fused aromatic structures, anthraquinone-based dyes are more resistant to biodegradation than azo-based dyes [46]. Acid Blue 25 (AB25), Disperse Red 11, and Reactive Brilliant Blue (RRB) are widely used anthraquinone dyes [47,48].

Triarylmethane dyes, also known as triphenylmethane dyes, are widely utilized in the textile industry. They are applied extensively to materials such as nylon, wool, cotton, and silk [49]. Furthermore, they are used in antimicrobial, antitubercular, and antifungal activities [50]. Triarylmethane dyes derive their main structure from a monomethine unit with three terminal aryl groups serving as chromophores, and functionalization is achieved through the use of auxochromic groups such as hydroxyl, amino, or dimethyl amino. Basic Fuchsin (BF), Malachite Green (MG), and Methyl Violet (MV) are the most commonly used triarylmethane dyes [51].

Table 1. Characteristics of widely used dyes.

Dye	Structure	Chemical Formula	MW * (g/mol)	Log K_{OW}	CAS Number	Reference
		Azo				
Aniline Yellow	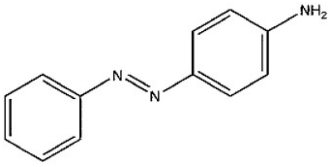	$C_{12}H_{11}N_3$	197.24	3.41	60-09-3	[52]
Reactive Orange 16	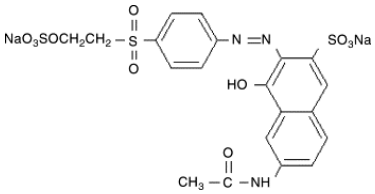	$C_{20}H_{17}N_3Na_2O_{11}S_3$	617.5	NR *	20262-58-2	[53]
Orange II	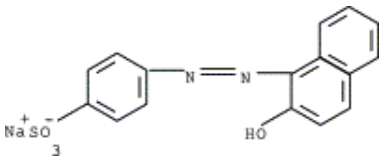	$C_{16}H_{11}N_2NaO_4S$	350.3	NR	633-96-5	[54]
Acid Orange 12	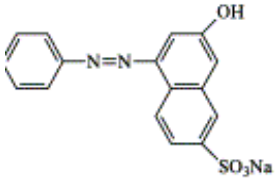	$C_{16}H_{11}N_2NaO_4S$	350.3	NR	1934-20-9	[55]
Congo Red	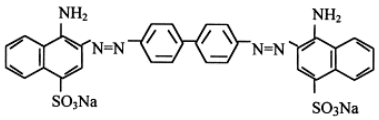	$C_{32}H_{22}N_6Na_2O_6S_2$	696.7	NR	573-58-0	[56]
Oil Red	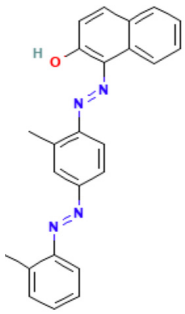	$C_{24}H_{20}N_4O$	380.4	NR	85-83-6	[57]

Table 1. *Cont.*

Dye	Structure	Chemical Formula	MW * (g/mol)	Log K_{OW}	CAS Number	Reference
Direct Blue-1	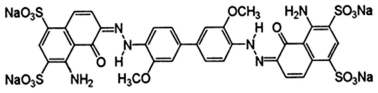	$C_{34}H_{24}N_6Na_4O_{16}S_4$	992.8	NR	2610-05-1	[58]
Reactive Black 5	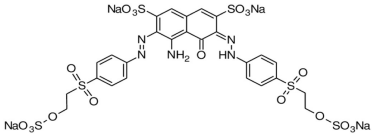	$C_{26}H_{21}N_5Na_4O_{19}S_6$	991.8	NR	17095-24-8	[59]
Sudan Black-B	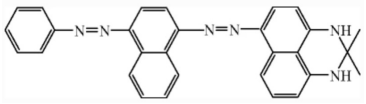	$C_{29}H_{24}N_6$	456.5	NR	4197-25-5	[60]
Direct Blue-71	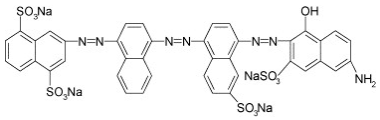	$C_{40}H_{23}N_7Na_4O_{13}S_4$	1029.9	NR	4399-55-7	[61]
Direct Black-22	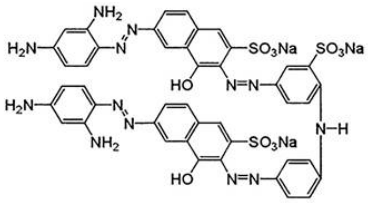	$C_{44}H_{32}N_{13}Na_3O_{11}S_3$	1084	NR	6473-13-8	[62]
		Phthalocyanines				
Reactive Blue 21	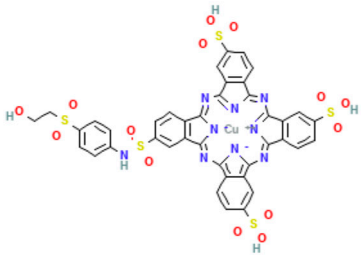	$C_{40}H_{25}CuN_9O_{14}S_5$	1079.6	NR	12236-86-1	[63]
Reactive Blue 7	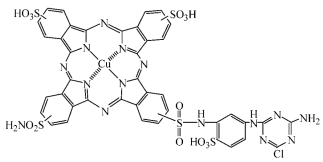	$C_{41}H_{24}CuN_{15}O_{13}S_5Cl$	1194.1	NR	-	[64]
		Xanthene				
Rhodamine B	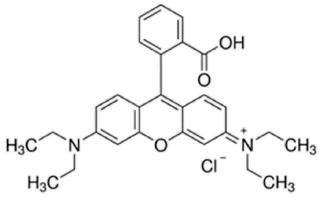	$C_{28}H_{31}ClN_2O_3$	479.0	NR	81-88-9	[65]

Table 1. *Cont.*

Dye	Structure	Chemical Formula	MW * (g/mol)	Log K_{OW}	CAS Number	Reference
Phloxine B	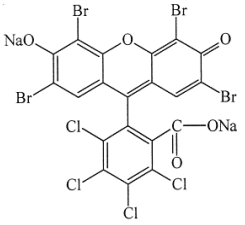	$C_{20}H_2Br_4C_{l4}Na_2O_5$	829.6	NR	18472-87-2	[66]
Erythrosine B	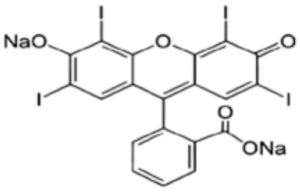	$C_{20}H_6I_4Na_2O_5$	879.9	NR	16423-68-0	[67]
		Nitro				
Picric Acid	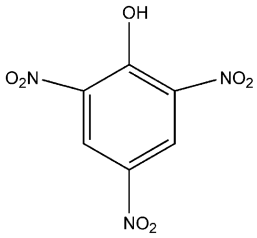	$C_6H_3N_3O_7$	229.10	1.44	88-89-1	[68]
Naphthol Yellow S	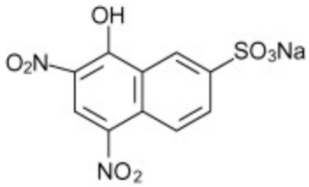	$C_{10}H_4N_2Na_2O_8S$	358.19	NR	846-70-8	[69]
Acid Orange 3	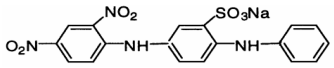	$C_{18}H_{13}N_4NaO_7S$	452.4	-0.69	6373-74-6	[70]
C.I. Disperse Yellow 42	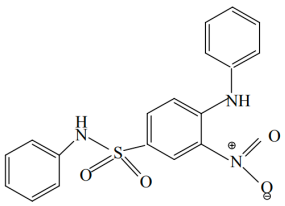	$C_{18}H_{15}N_3O_4S$	369.4	NR	5124-25-4	[71]
C.I. Disperse Yellow 70	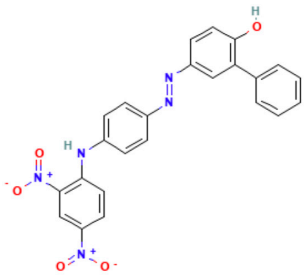	$C_{24}H_{17}N_5O_5$	455.4	NR	12223-91-5	[72]

Table 1. *Cont.*

Dye	Structure	Chemical Formula	MW * (g/mol)	Log K_{OW}	CAS Number	Reference
		Quinoline				
Quinoline Yellow	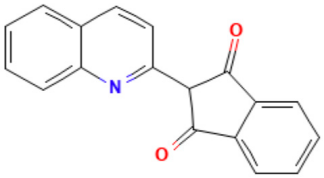	$C_{18}H_{11}NO_2$	273.3	4.10	8003-22-3	[73]
		Indigo				
Indigo Carmine	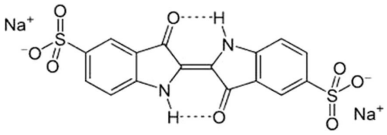	$C_{16}H_8N_2Na_2O_8S_2$	466.4	NR	860-22-0	[74]
		Acridine				
Acridine Orange	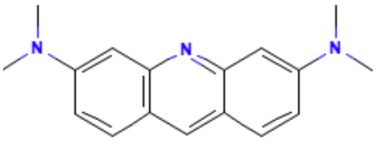	$C_{17}H_{20}ClN_3$	301.8	NR	65-61-2	[75]
Acridine Yellow G	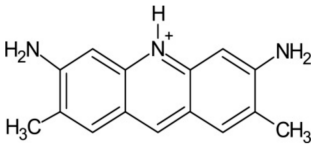	$C_{15}H_{16}ClN_3$	273.76	NR	135-49-9	[76]
		Azine				
Methylene Blue	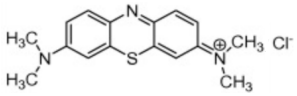	$C_{16}H_{18}N_3ClS$	319.8	0.75	61-73-4	[77]
Thionin	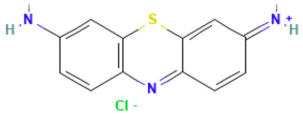	$C_{12}H_{10}ClN_3S$	263.75	NR	581-64-6	[78]
Safranin O	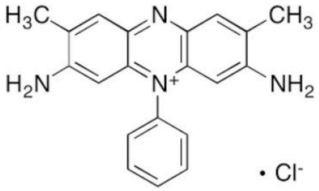	$C_{20}H_{19}ClN_4$	350.85	NR	477-73-6	[79]
		Anthraquinone				
Acid Blue 25	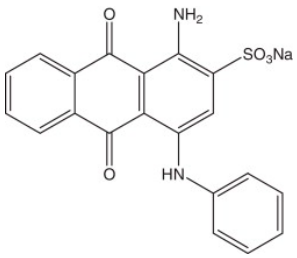	$C_{20}H_{13}N_2NaO_5S$	416.4	NR	6408-78-2	[80]

Table 1. *Cont.*

Dye	Structure	Chemical Formula	MW * (g/mol)	Log K_{OW}	CAS Number	Reference
Disperse Red 11	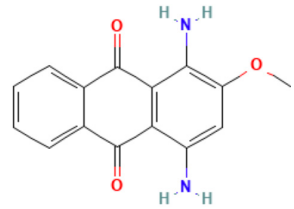	$C_{15}H_{12}N_2O_3$	268.27	NR	2872-48-2	[81]
Reactive Brilliant Blue		$C_{22}H_{16}N_2Na_2O_{11}S_3$	626.5	NR	2580-78-1	[82,83]
		Triarylmethane				
Basic Fuchsin	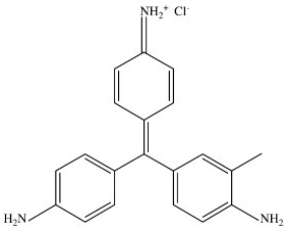	$C_{20}H_{20}ClN_3$	337.8	NR	632-99-5	[84]
Malachite Green	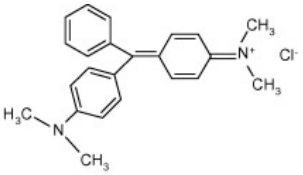	$C_{23}H_{25}N_2Cl$	364.92	0.62	569-64-2	[85]
Methyl Violet	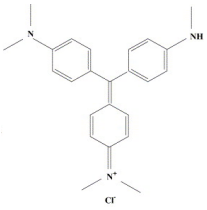	$C_{25}H_{30}ClN_3$	408.0	0.51	548-62-9	[86,87]

* MW = Molecular weight; NR = not reported.

3. Toxicity of Dyes on Aquatic Environments

Industrial dyes in high concentrations in water sources reduce the water's ability to reoxygenate and block sunlight, disrupting the biological activity of aquatic life and the photosynthesis of aquatic plants or algae. The harm caused to the aquatic environment can persist for a long time (several years of half-life) and lead to toxic effects, accumulation in aquatic organisms such as fish, decomposition into carcinogenic or mutagenic compounds, and low aerobic biodegradability [88]. According to Gita et al. [88], a comparative toxicological study of textile dye wastewater on *Gambusia affinis*, a freshwater fish, revealed significant cytotoxic effects. Additionally, there was a decrease in fish counts and changes in shape (poikilocytosis) and size. Apart from that, the presence of dye in a body of water adversely affects the health of algae in terms of growth, protein content, pigment content, and nutrient content [88]. Hernández-Zamora et al. [89] reported that Congo Red (CR) could significantly inhibit the growth of *Chlorella vulgaris*, microalgae. The exposure to indigo dye resulted in a decrease in the growth rate and biomass production of *Scenedesmus quadricauda* [90]. This is likely due to the presence of humic substances, which disrupt

the internal environment's homeostasis and cause irreversible damage by compromising biological processes [91].

In addition, dyes can become carcinogenic when degraded by microbes in biological systems such as animals and humans. It is essential to treat effluent containing dyes before releasing it into water sources to minimize impact and prevent further strain on water bodies. Most dyes are xenobiotics, making conventional removal methods ineffective [92].

In toxicity studies, EC_{50} refers to the concentration of a substance that produces a half-maximum response [93]. LC_{50} tests measure the concentration of a toxic substance in water that can kill 50% of the tested fish or microorganisms. Therefore, in Table 2, different toxicity tests of dyes on aquatic organisms based on the values of LC50/EC50 are compared. As shown in Table 2, methylene blue is more toxic to *S. platensis* compared with other dyes and microalgae species. Krishna Moorthy et al. [90] found that even at lower concentrations, methylene blue remains toxic compared to other dyes and studies. The toxicity of microalgae exposed to the dye may be due to factors such as the chemical structure of the colorants, the duration of exposure, and the conditions in which they are exposed [90]. Based on the Table 2, the fathead minnow is so sensitive to exposure to Sudan Red G and Disperse Yellow 7.

Table 2. Toxicity of different dyes on fish and algae.

Dye	Dye Category	Species	EC50 or LC50 (mg/L)	Remark	Reference
			Algae		
Rhodamine B	Xanthene	*Raphidocelis subcapitata*	14	EC50 reported for 72 h exposure to dye.	[94]
Reactive Orange 16 Congo Red	Azo	*S. capricornutum*	7.8 4.8	EC50 reported for 96 h exposure to dye.	[95]
Optilan red	Azo	*Chlorella vulgaris*	23.1	EC50 reported for 96 h exposure to dye.	[96]
Methylene blue	Azine	*Chlorella vulgaris* *S. platensis*	61.8 to 5.4 5.8 to 1.0	EC50 reported for 24 to 96 h exposure to dye.	[90]
Reactive red 114 Basic red 14	Azo Xanthene	*Chlorella vulgaris*	95.5 10.8	EC50 reported for 96 h exposure to dye.	[97]
Optilan red	Azo	*Spirulina platensis*	7.6	EC50 reported for 96 h exposure to dye.	[91]
			Fish		
Rhodamine B	Xanthene	*Danio rerio*	18	LC50 reported for 72 h exposure to dye.	[94]
Malachite green	Triarylmethane	*Lepormis macrochirus* *Ictarulus punctatus*	2.1 0.2 to 1.3	LC50 reported for 6 h exposure to dye.	[98]
Remazol gelb-GR	Azo	Zebrafish embryos	151.9	LC50 reported for 96 h exposure to dye.	[99]
Trypan blue	Azo	*C. mrigala*	40	LC50 reported for 96 h exposure to dye.	[100]
Sudan Red G Disperse Yellow 7	Azo	Fathead minnow (*P. promelas*)	0.02 0.01	-	[101]

4. Membrane Bioreactor (MBR) for Removal of Dyes

The integration of membrane separation (mostly microfiltration—MF and ultrafiltration—UF) and biological degradation processes in various conditions (aerobic, anoxic, and anaerobic) has demonstrated promising potential in treating contaminated wastewaters over the past 20 years [102]. MBR systems use membrane filtration units with

different pore sizes, either within biological tanks or installed separately, to effectively separate clear wastewater from suspended solids, which are kept within the wastewater treatment plant (WWTP) [103]. Membrane materials can be grouped into three main categories: polymer, ceramic, and metallic [104].

Polyvinylidene fluoride (PVDF), polystyrene (PS), polysulfone (PSF), polyetherimide (PEI), polyacrylonitrile (PAN), cellulose acetate (CA), polyethylene (PE), and polyethersulfone (PES) are commonly used in polymeric membranes [105]. The main benefit of polymeric MBR is that it is cost-effective compared to ceramic and metallic options; however, polymeric membranes have some limitations, such as excessive fouling and lower stability under challenging operating conditions such as salt [106].

Ceramic membranes have seen wide use in water treatment, gas purification, and product concentration. However, their high fabrication cost makes them a challenge to implement on a large commercial scale [107]. Ceramic membranes have certain advantages over polymeric membranes because of their inorganic matrix and specific micro- and nanostructural properties. They offer long-term stability at high temperatures, exceptional chemical stability against acids and solvents, mechanical stability under high pressure, and a long service life, making them suitable for use in harsh environments [108].

Metallic membranes can be manufactured using different methods, including electroplating, chemical vapor deposition (CVD), physical vapor deposition (PVD), electroless plating, and sintering. The resulting metallic membranes come in different shapes, such as disks and tubes, and can be customized in terms of size to meet specific needs [109]. Typically, metallic membranes are preferred for applications in harsh environments (e.g., high temperatures, high chemical concentrations).

The treatment of most dyes, such as azo dyes, is challenging through aerobic methods due to their recalcitrant and toxic nature to microorganisms. However, under anaerobic conditions, azo dyes serve as electron acceptors and can be easily broken down into aromatic amines, making anaerobic bioreactors more effective for removing color [110]. Therefore, the AnMBR has been considered in this study. Anaerobic digestion (AD) is a process where facultative anaerobic bacteria break down biodegradable organic matter in anaerobic conditions, resulting in the production of biogas. This method is more energy-efficient, degrades organic matter effectively, and produces less biosolids compared to methods that require oxygen [111].

According to Ji et al. [112], anaerobic biological treatment can eliminate emerging contaminants (ECs) from wastewater. However, conventional anaerobic digestion technology has limitations in removing hydrophilic and toxic ECs due to low biomass levels. Furthermore, the stability and functional microbial community in the conventional AD system are vulnerable to the toxicity of ECs [112]. The AnMBR system, compared to conventional anaerobic digestion process technology, has a higher biomass and a longer sludge retention time (SRT) because of the membrane module's role [113].

As described by Ji et al. [112], AnMBR technology (Figure 1) can be categorized into three forms based on how the membrane module is incorporated into the bioreactor: side-stream AnMBR (SS-AnMBR), submerged AnMBR (S-AnMBR), and external submerged AnMBR (ES-AnMBR). SS-AnMBR involves placing the membrane module outside the bioreactor and pumping the treated wastewater at a high flow rate to the outer membrane module for separation. S-AnMBR has the membrane module submerged in the bioreactor, and the clean water is separated from the reactor through vacuum, which is commonly used in industrial wastewater treatment, such as in the textile industry. ES-AnMBR is mainly employed in the treatment of municipal sewage and has the membrane module submerged in an external chamber. Apart from that, some novel AnMBRs (such as the dynamic AnMBR, the AnDMBR) have been applied.

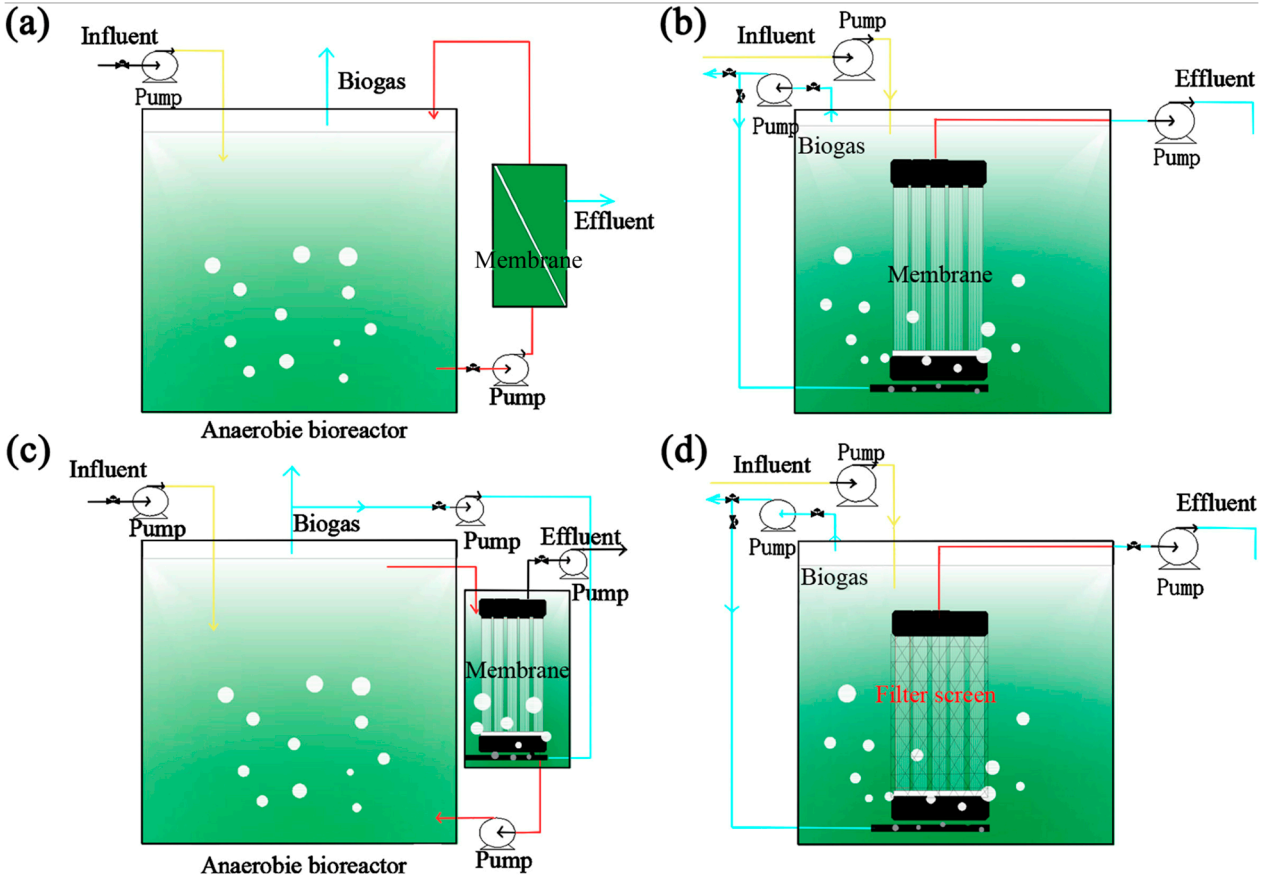

Figure 1. Fundamental schematics of conventional AnMBR: (**a**) SS-AnMBR, (**b**) S-AnMBR, (**c**) ES-AnMBR, and (**d**) AnDMBR. (Source: [112]; copyright permission received on 15 February 2023, from Elsevier).

As mentioned above, novel AnMBRs are frequently applied in the treatment of industrial wastewater. Most reported novel AnMBRs are anaerobic electrochemical membrane bioreactors (AnEMBRs), anaerobic dynamic membrane bioreactors (AnDMBRs), anaerobic membrane distillation bioreactors (AnMDIBRs), and anaerobic biofilm membrane bioreactor (ABMBR) [114].

AnDMBR (Figure 1d) is a technology designed to improve performance and is more affordable than AnMBRs. It uses a low-cost support structure, such as coarse cloth or mesh with a 10–100 µm pore size, on which a biofilm layer develops. Wastewater is filtered through this dynamic membrane, retaining suspended solids in the bioreactor. AnDMBRs use less energy-intensive fouling mitigation strategies such as backwashing and relaxation rather than sparging [115].

Researchers are developing the AnEMBR (Figure 2) to improve the performance of AnMBRs by combining membrane separation, anaerobic microbiology, and microbial electrolysis cell technology for better control of membrane fouling and increased contaminants removal. The membrane reduces sludge loss when an electrical bias is applied to the membrane surface, creating electrochemical conditions that help alleviate membrane fouling through electrostatic forces, electro-flocculation, electrochemical reactions, and the scouring effect of gas produced by the electrode [114].

Anaerobic membrane distillation bioreactors (AnMDIBRs, Figure 3) use hydrophobic membranes and temperature differences for efficient wastewater treatment and reuse. The mass transfer in AnMDIBRs is driven by temperature differences, allowing for water vapor to evaporate through the membrane and improve effluent quality [114].

The anaerobic biofilm membrane bioreactor (AnBMBR) combines the advantages of a conventional MBR process, such as a minimal physical footprint, efficient solid-liquid

separation, low sludge generation, and more, with the added benefit of utilizing biofilm to enhance pollutant removal. This is due to the high density of biomass and diverse biological environment within the biofilm, as well as the favorable conditions it creates for microorganisms to thrive [116]. In AnBMBR, certain carriers are utilized for the growth of microorganisms. These carriers enhance mass transfer and foster the growth of biofilms [117].

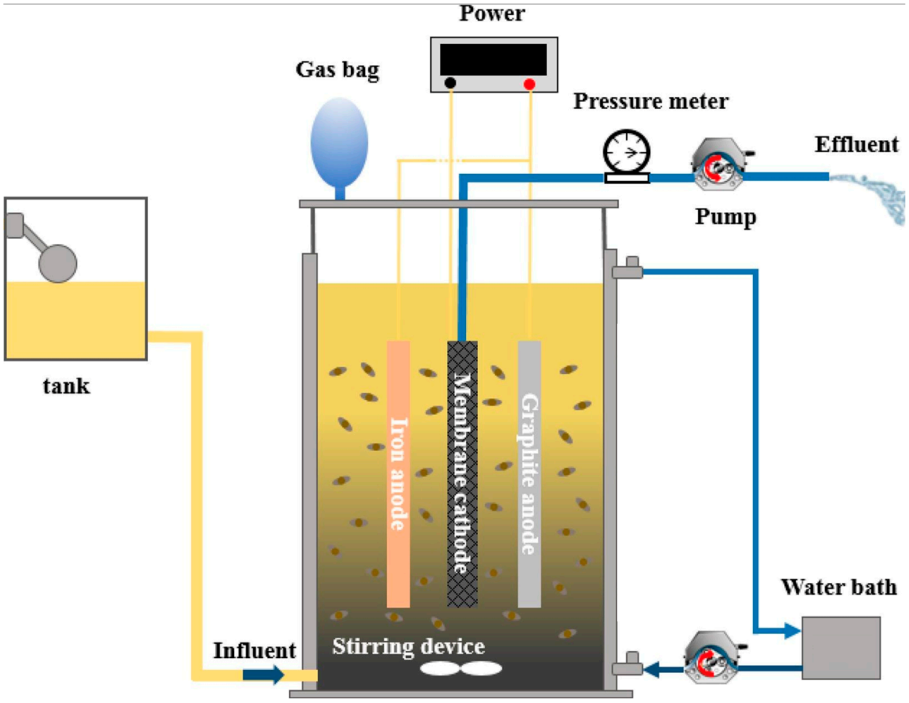

Figure 2. Schematic of AnEMBR. (Source: [118]; copyright permission received on 15 February 2023, from Elsevier).

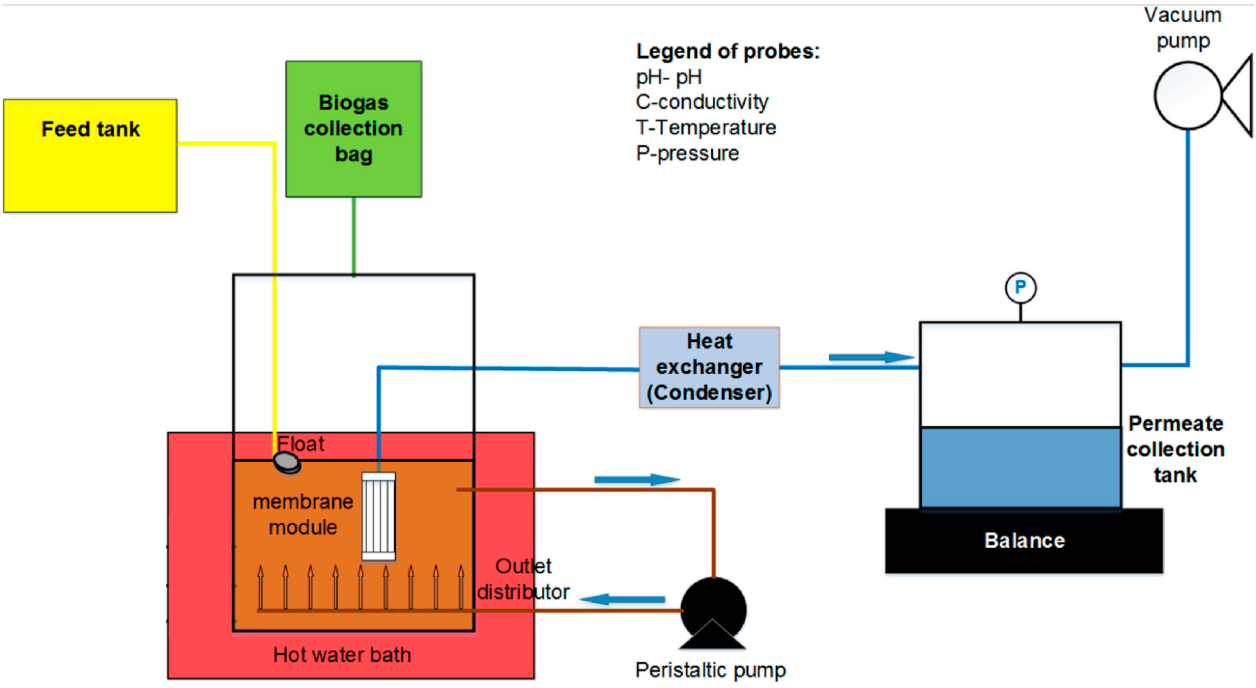

Figure 3. Schematic of AnMDIBRs. (Source: [119]; copyright permission received on 15 February 2023, from Elsevier).

Several studies [120,121] have indicated that AnMBRs are highly effective in eliminating nutrients and organic contaminants from water. Ramadan et al. [122] found that AnMBRs were able to remove more than 95% of the chemical oxygen demand (COD) when operated at a temperature of 35 °C. The study also showed that the hydraulic retention time (HRT) and solid retention time (SRT) were 9–16 days and 365 days, respectively. An anaerobic biofilm membrane bioreactor (ABMBR) was utilized to effectively eliminate 95% of the chemical oxygen demand (COD) from wastewater. The hydraulic retention time (HRT) was set at 1 day, and the system was operated at a temperature of 35 °C [123]. Keerthi et al. [124] used a hybrid membrane bioreactor (HMBR) with integrated electrocoagulation to remove 90% of the COD and 93% of color from tannery wastewater, while the membrane bioreactor alone was able to remove 73% of the COD and 76% of the color from tannery wastewater. In another study, a dynamic membrane bioreactor (DMBR) was used to remove 91% of the COD and over 97% of dye from textile wastewater when HRT and dye concentration were 1–2 d and <200 mg/L, respectively, at temperature 32–34 °C [125]. According to Sari Erkan et al. [126], a moving bed membrane bioreactor (MBMBR) was found to be highly effective in removing contaminants, achieving a 98% removal of chemical oxygen demand (COD) and 89.5% removal of color. The STR was set at 30 days, and the HRT was between 15.2 and 16.5 days. Table 3 summarizes the literature on the removal of dyes with AnMBR. AnDMBR was performed, using nylon mesh support material with pore sizes ranging from 20 µm to 100 µm, to remove 99% of the color [127]. Katuri et al. [128] used AnEMBR, with nickel-based hollow-fiber membranes, for treating organic aqueous solutions. They found that more than 97% of COD was removed when the voltage was between 0.5 and 0.9 V and the current was below 25 mA at a temperature of 25 °C. According to Li et al. [123], an AnBMBR was able to reduce 95% of COD from wastewater.

Table 3. The performance of AnMBR in the removal of dyes.

Dye	Water Bodies	Removal (%)	Treatment	Cleaning	Operation Condition	Reference
Azo (Black 5, Black WNN, and Red 3BS	Synthetic wastewater	79.9	* HAnMBR (SBR-AnMBR)	* NR	HRT = 48 h; concentration of color = 80 mg/L; Temperature = 30 °C	[129]
Methylene blue, Cibacron blue, and Cibacron yellow	Synthetic wastewater	99.0	Modified AnMBR (anaerobic membrane distillation bioreactor)	Physical (Backwash)	Polymeric membrane (polytetrafluoroethylene-PTFE and polypropylene-PP); color concentration = 1000 Pt.Co; Temperature > 35 °C; HRT = 12 h	[130]
Methylene blue, Cibacron blue, and Cibacron yellow	Synthetic wastewater	92.3	Modified AnMBR (Anaerobic Forward Osmosis Membrane Bioreactor (An-FOMBR))	Chemical (NaOCl)	Polymeric membrane (polyamide-PA and polysulfone-PSF); HRT = 12–24 h; Temperature = 36 °C; SRT = 60 days; color concentration of color = 1000 Pt. Co.	[131]
Methyl orange	Synthetic wastewater	100	Modified AnMBR (methane-based hollow fiber membrane bioreactor)	NR	HRT = 1.5–2 days; Polymeric membrane (polyvinylidene fluoride-PVDF); concentration of MO = 400 mg/L	[132]
Methyl orange	Synthetic wastewater	100	Modified AnMBR (anaerobic baffled membrane bioreactor)	Physical and chemical (HCl)	HRT = 15–17 h; Polymeric membrane; concentration of MO = 50 mg/L	[133]

Table 3. *Cont.*

Dye	Water Bodies	Removal (%)	Treatment	Cleaning	Operation Condition	Reference
Reactive orange 16	Synthetic wastewater	97	HAnMBR (integrated with ozonation)	NR	HRT = 12 h; 30 min ozonation; temperature = 22–25 °C	[134]
Reactive orange 16	Synthetic wastewater	61	AnMBR	NR	HRT = 12 h; Dye concentration = 5 mg/L; temperature = 22–25 °C	[134]
Reactive Black 5	Synthetic wastewater	95	HAnMBR (integrated with downflow hanging sponge)	Physical and chemical (NaOCl)	HRT = 12–24 h; temperature = 30 °C; polymeric membrane; dye concentration = 50 mg/L	[135]
Mostly azo dyes	Real dying wastewater	>90	Modified AnMBR (Anaerobic flat-sheet ceramic membrane bioreactor)	Physical and chemical (NaOCl)	HRT = 24 h; Ceramic membrane; temperature 34 °C	[136]
Remazol Brillant Violet 5R	Synthetic wastewater	97	DMBR	Physical (Vacuum line)	HRT = 11.2 h–14.5 h; polymeric membrane (PVC); dye concentration = 50 mg/L; temperature 34 °C; SRT = 60 days	[137]
Dyes	Textile wastewater	Up to 87	S-AnMBR	NR	HRT = 12 h–24 h; polymeric membrane; dye concentration = 50 mg/L; temperature 35 °C	[138]
Navy blue	Real dying wastewater	99	Modified AnMBR (Hydrolysis acidification flat-sheet ceramic membrane bioreactor)	Chemical (pumping 1000 mg/L NaOCl into the inner space of the membranes)	HRT = 12 h; Ceramic membrane; temperature 34 °C	[139]

* SBR—sequencing batch reactor; NR—not reported.

According to Table 3, the hybrid AnMBR and the modified AnMBR are more effective at removing dyes. In addition, many AnMBRs were operated at high temperatures (above 30 °C) to maintain the biological process. Furthermore, the primary cleaning method was physical, followed by chemical cleaning using NaOCl.

4.1. Removal Mechanisms and Vital Factors

In AnMBRs, there are two primary methods for removing dyes: physical treatment through membrane filtration (Figure 4) and biological treatment through the use of microbial communities [140].

The membrane's performance is dependent on various factors, such as pore size, material composition, wastewater characteristics, solubility, and retention time. Retention occurs as a result of the concentration difference between the retentate (the portion of the solution that cannot pass through the membrane) and the permeate (the solution that has been filtered) [141]. The molecular weight of dyes varies widely, ranging from 265 to 1419 g/mol for Acridine Orange and Reactive Green 19, respectively. This characteristic is of utmost importance for wastewater treatment technologies, as it can significantly impact the process performance in a positive or negative manner [142]. For instance, membrane rejection mechanisms may occur through size exclusion, where the membrane's ability to retain a molecule of a particular compound is determined by the fraction of membrane pores that are smaller than the molecule's size [143]. As a result, dyes with a higher molecular

weight are more readily retained by the sieving effect of the membranes [144]. Additionally, other removal mechanisms such as electrostatic repulsion/attraction or adsorption can influence the membrane's efficiency. Therefore, the efficacy of the filtration system is also determined by the physicochemical properties of the dyes and the membrane characteristics, such as the average pore size, molecular weight cut-off (MWCO), and surface charges [142]. A research study employed a self-prepared thin-film composite NF membrane, which was created through interfacial polymerization on the surface of a dual-layer hollow fiber membrane, to remove dyes from textile wastewater. The results of the study revealed that the membrane surface's physical and chemical properties led to a rejection rate of more than 99% as it interacted with the positive and negative groups of reactive dyes [145]. According to Ding et al. [146], during dye filtration, the permeate flux of membranes was found to be lower than the permeability of the membranes for pure water. This phenomenon is attributed to the adsorption of dye on the surfaces and pore walls of the membrane [146]. Zhong et al. [147] conducted a study in which they utilized an NF membrane to eliminate dye from textile wastewater. The NF membranes had a mean effective pore diameter ranging from 1.13 to 1.20 nm, a molecular weight cutoff (MWCO) of 1627–1674 Da, and a high pure water permeability (PWP) of 9–14 LMH bar^{-1}, which demonstrated effective performance in removing dye [147].

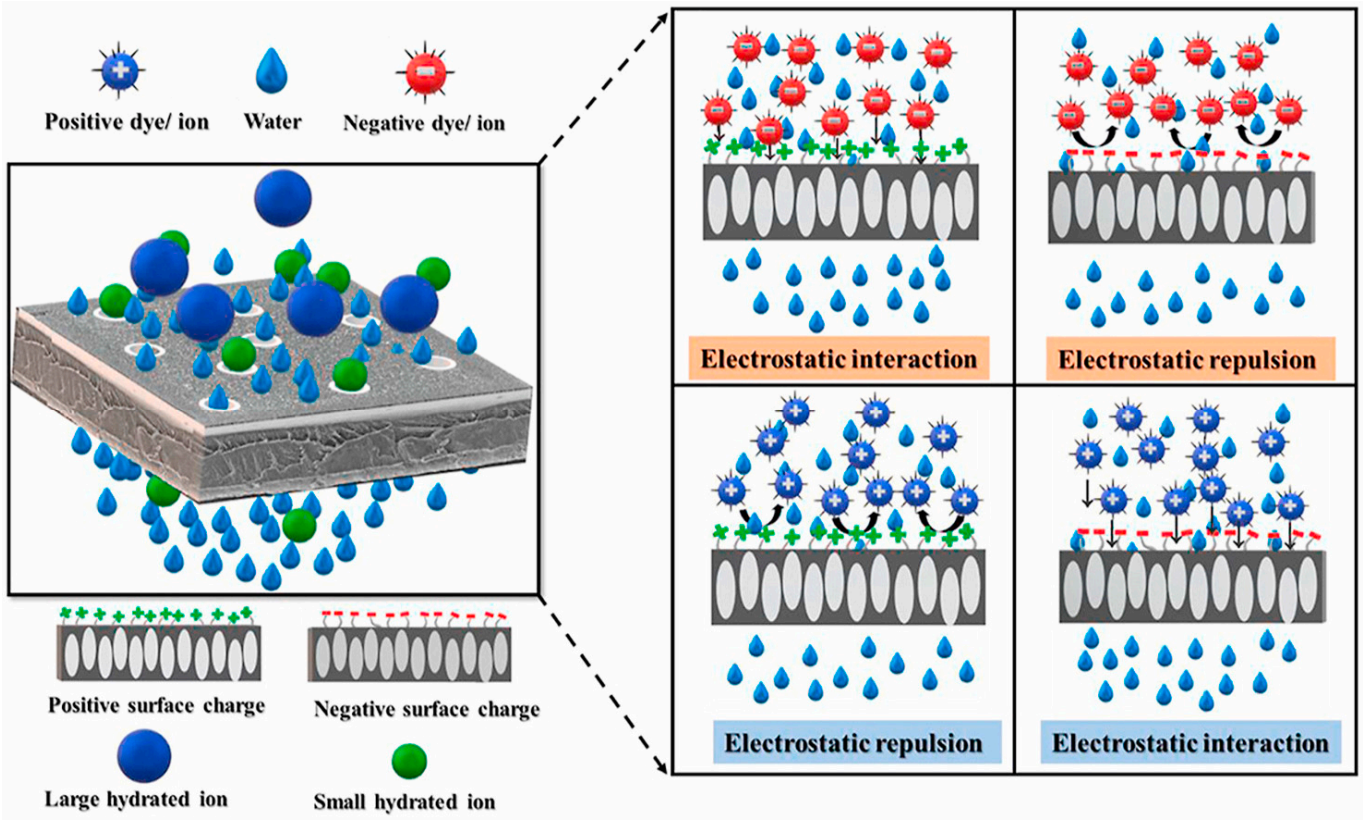

Figure 4. Schematic of dye removal with membrane process. (Source: [148]; copyright permission received on 15 February 2023, from Elsevier).

In terms of the biological process of dye removal, several studies have demonstrated the potential usefulness of anaerobic reductive cleavage of the dyes bonds by microbes. Some of these studies have utilized anaerobic activated sludge, while others have employed mixed bacterial cultures [149]. As stated by Türgay et al. [150], due to their unique properties, anaerobic microorganisms are often the preferred choice for decolorizing certain dyes present in textile wastewaters. One notable example is their ability to generate electrons that can effectively cleave the azo bond. Khalili and Bonakdarpour utilized a bacterial consortium (activated sludge) to remove dye under anaerobic conditions [151]. Fang et al. [152]

conducted a study in which a membrane bioreactor inoculated with activated sludge (a bacterial consortium) successfully removed a significant amount of dye. One key factor that contributes to the effectiveness of AnMBRs is the unique bacterial communities that are present in these systems. These bacteria play an essential role in breaking down the dye molecules and converting them into less harmful substances.

In one study conducted by Zhou et al. [153], the top three dominating phyla in AnMBRs were found to be *Chloroflexi*, *Euryarchaeota*, and *Firmicutes*, with other phyla such as *Proteobacteria*, *Nitrospirae*, *Bacteroidetes*, and *Chlorobi* also commonly detected under diverse conditions. According to a different study, the dominant phyla in an AnMBR were *Bacteroidetes* and *Firmicutes*, which are known for their ability to degrade organics [154]. According to Liao et al., *Firmicutes*, *Chloroflexi*, *Bacteroidetes*, and *Proteobacteria* are commonly identified as the dominant bacterial phyla in anaerobic systems [155]. Chaudhari et al. [156] confirmed the prevalence of the *Firmicutes*, *Proteobacteria*, and *Bacteroidetes* phyla during different stages of dye wastewater treatment.

Maintaining a stable granular structure is crucial in anaerobic systems, and *Chloroflexi*, a strictly anaerobic bacterium, plays a vital role in this process. Studies have reported that *Chloroflexi* can degrade starch into acetate and other short-chain fatty acids, which can then be utilized by methanogens [157]. The presence of electrochemically active bacteria that can transfer electrons, such as *Firmicutes*, *Acidobacteria*, and *Actinobacteria*, is crucial in the removal of dye under anaerobic conditions [158]. Chaudhari et al. [156] stated that with continuous exposure to the dye, there was a notable increase in the relative abundance of *Firmicutes*. This suggests that *Firmicutes* may have played a significant role in the decolorization of reactive blue HERD dye [156]. In addition, Qiu et al. [159] stated that bacteria classified under the *Firmicutes* phylum are accountable for breaking down aromatic amines into CO_2 and alkenes. Additionally, a majority of *Firmicutes* bacteria demonstrate heterotrophy and can facilitate the production of electron equivalents, suggesting that they can enhance the decolorization of azo dyes by breaking down aromatic intermediates [159].

The significant role that some *Bacteroidetes* play in breaking down complex molecules into simpler ones within the host intestine implies that these bacteria may also have a crucial function in the bioconversion of complex molecules into simpler ones during anaerobic processes [160]. In addition, *Bacteroidetes* are capable of extracellular electron transfer, which could be linked to the process of methanogenesis in anaerobic systems. Within anaerobic sludge, these bacteria may be involved in the direct transfer of electrons between species during azo dye reduction [155]. The *Proteobacteria* phylum possesses the capability to break down complex carbon sources, and a majority of these bacteria are either obligate or facultative anaerobes that are commonly found in anaerobic reactors [155]. Within the *Proteobacteria*, *Alphaproteobacteria*, *Betaproteobacteria*, *Deltaproteobacteria,* and *Gammaproteobacteria* are mostly reported in dye removal processes under anaerobic conditions [161].

4.2. Fouling and Cleaning

In AnMBR technology's application to waste and wastewater treatment, membrane fouling is the most significant challenge, encompassing various parameters such as sludge concentration, HRT, soluble metabolic products, and extracellular polymeric substances [162]. The main issue in the MBR process is fouling of membranes (Figure 5), which causes decline in permeate flux, an increase in trans-membrane pressure, and higher operating costs for cleaning. Fouling occurs due to organic, inorganic, particulate, and biofouling, and is influenced by wastewater and biomass composition [140].

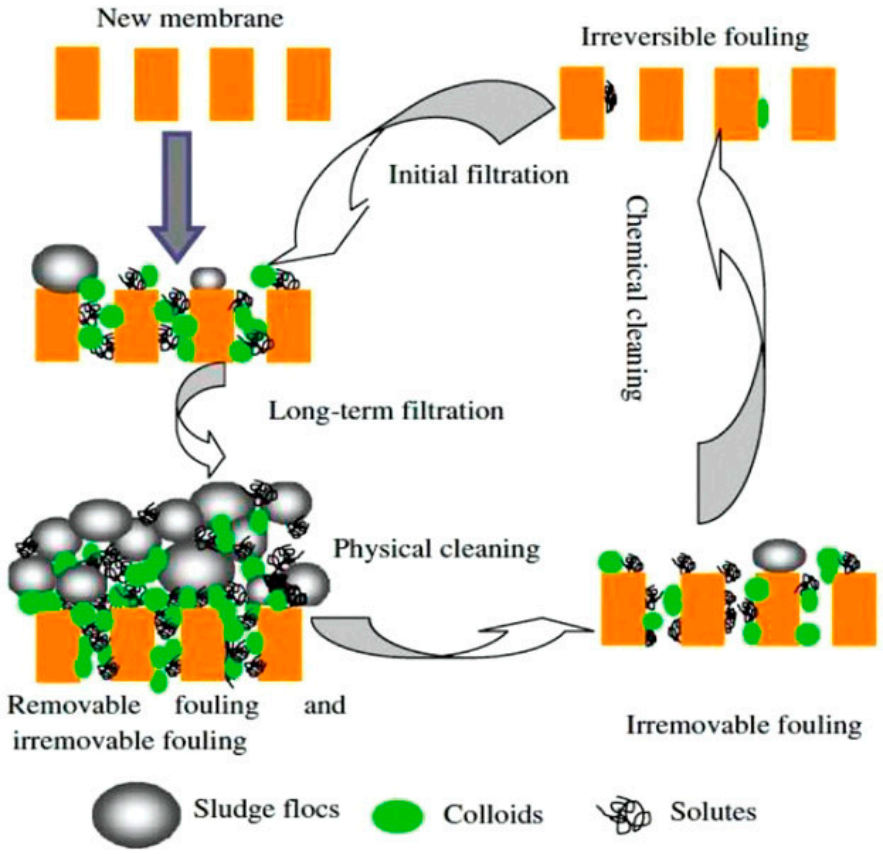

Figure 5. Basic diagram outlining the process of fouling in MBRs, as well as the methods used for its removal. (Source: [163] copyright permission received on 15 February 2023, from Wiley).

Figure 6 shows the AnMBR fouling classifications. External fouling takes place when particles, colloids, and macromolecules larger than the membrane's pore size deposit on the surface. Internal fouling is caused by the presence of small particles, solutes, and undissolved matter that are retained or submerged within the membrane pores [113]. Fouling of the membrane can also be differentiated into two further types, reversible and irreversible, based on the ease of cleaning [104]. According to Maaz et al. [113], irrecoverable fouling occurs over a long-term experiment, where once the membrane is fouled, its original permeability can never be regained. Residual fouling, on the other hand, involves the buildup of fat, protein, and minerals that can be attributed to various fouling mechanisms [164]. Biofouling refers to the interaction of components of the biological treatment broth with the membrane surface [113].

Membrane cleaning methods are mainly categorized as physical and chemical based on the membrane materials, foulant composition, and nature of cleaning reagents used [165]. In addition to physical cleaning (e.g., backwash and in-line ultrasonic), chemical cleaning is a widely used method to clean polymeric membranes. Chemical cleaning agents can be divided into seven categories, including acids (e.g., nitric acid, sulfuric acid), alkalis (e.g., carbonates, hydroxides), caustics (e.g., sodium hydroxide), disinfectants (e.g., hydrogen peroxide, chlorine, sodium hypochlorite, peroxyacetic acid, metabisulfite), enzymes (e.g., proteases, lipases), sequestrants (e.g., ethylenediaminetetraacetic acid), and surfactants (e.g., sodium dodecyl sulfate, alkyl sulfate) [166]. Backwashing is a more effective cleaning method for ceramic membranes, reducing the risk of concentration polarization, cake layer formation, and fouling [167]. Physical cleaning methods are ineffective in treating irreversible fouling, and therefore, the efficiency (flux) of the membrane can only be restored through chemical cleaning [165].

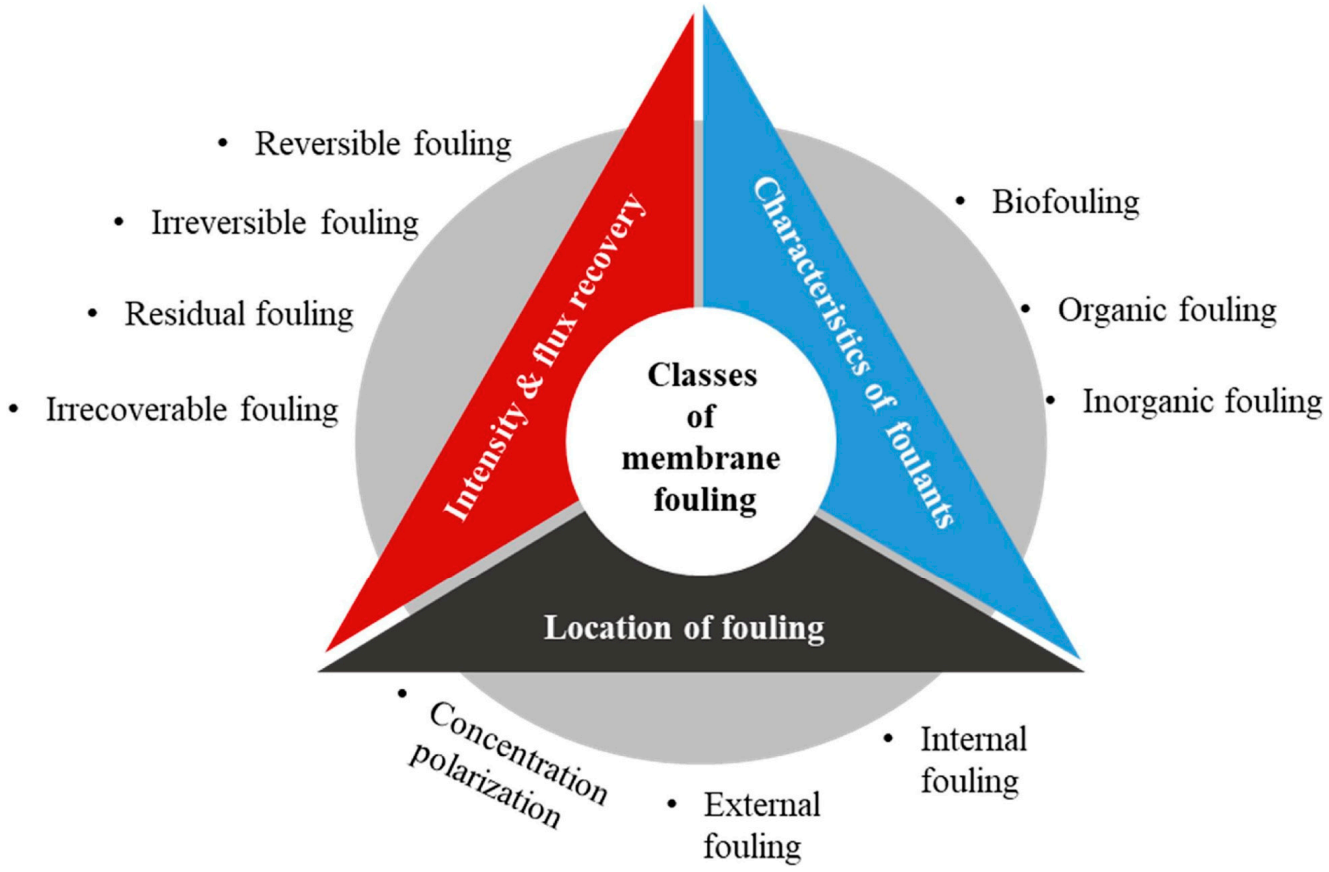

Figure 6. AnMBR fouling classifications. (Source: [113]; copyright permission received on 15 February 2023, from Elsevier).

5. Conclusions

The presence of dyes in aquatic environments can have harmful effects on aquatic life. Azo, phthalocyanine, and xanthene are among the most commonly used dyes in industrial processes and have been identified as some of the most commonly occurring dyes in water bodies. Testing for the toxicity effect of dyes on aquatic organisms based on LC_{50} and EC_{50} measurements demonstrates their harmful effects on aquatic organisms. Anaerobic membrane bioreactors (AnMBRs) have emerged as a promising hybrid method for removing dyes from water bodies. However, fouling has been identified as a significant drawback of AnMBRs, and innovative designs and techniques are required to address this issue. This review provides insights into the challenges and future perspectives of AnMBRs in the removal of dyes from aquatic environments. The findings of this study can be valuable for researchers and practitioners working in the fields of wastewater treatment and environmental protection.

Author Contributions: Conceptualization, A.M.; validation, A.M.; investigation, A.M.; resources, A.M. and J.L.Z.; writing—original draft preparation, A.M., J.L.Z. and B.K.; writing—review and editing, A.M., J.L.Z., B.K., E.R. and N.K. All authors have read and agreed to the published version of the manuscript.

Funding: This research received no external funding.

Data Availability Statement: Not applicable.

Conflicts of Interest: The authors declare no conflict of interest.

References

1. Zhang, H.; Li, H.; Gao, D.; Yu, H. Source identification of surface water pollution using multivariate statistics combined with physicochemical and socioeconomic parameters. *Sci. Total Environ.* **2022**, *806*, 151274. [CrossRef] [PubMed]
2. Arif, M. Extraction of iron (III) ions by core-shell microgel for in situ formation of iron nanoparticles to reduce harmful pollutants from water. *J. Environ. Chem. Eng.* **2023**, *11*, 109270. [CrossRef]
3. Wang, M.; Janssen, A.B.G.; Bazin, J.; Strokal, M.; Ma, L.; Kroeze, C. Accounting for interactions between Sustainable Development Goals is essential for water pollution control in China. *Nat. Commun.* **2022**, *13*, 730. [CrossRef] [PubMed]
4. Kumar, V.; Thakur, C.; Chaudhari, P.K. Anaerobic biological treatment of dye bearing water in anaerobic sequencing batch reactor: Performance and kinetics studies. *J. Indian Chem. Soc.* **2022**, *99*, 100673. [CrossRef]
5. Naseem, K.; Farooqi, Z.H.; Begum, R.; Irfan, A. Removal of Congo red dye from aqueous medium by its catalytic reduction using sodium borohydride in the presence of various inorganic nano-catalysts: A review. *J. Clean. Prod.* **2018**, *187*, 296–307. [CrossRef]
6. Blanchard, R.; Mekonnen, T.H. Synchronous pyrolysis and activation of poly (ethylene terephthalate) for the generation of activated carbon for dye contaminated wastewater treatment. *J. Environ. Chem. Eng.* **2022**, *10*, 108810. [CrossRef]
7. Mahmood, K.; Amara, U.; Siddique, S.; Usman, M.; Peng, Q.; Khalid, M.; Hussain, A.; Ajmal, M.; Ahmad, A.; Sumrra, S.H.; et al. Green synthesis of Ag@CdO nanocomposite and their application towards brilliant green dye degradation from wastewater. *J. Nanostruct. Chem.* **2022**, *12*, 329–341. [CrossRef]
8. Ajmal, M.; Siddiq, M.; Aktas, N.; Sahiner, N. Magnetic Co–Fe bimetallic nanoparticle containing modifiable microgels for the removal of heavy metal ions, organic dyes and herbicides from aqueous media. *RSC Adv.* **2015**, *5*, 43873–43884. [CrossRef]
9. Benny, C.K.; Chakraborty, S. Dyeing wastewater treatment in horizontal-vertical constructed wetland using organic waste media. *J. Environ. Manag.* **2023**, *331*, 117213. [CrossRef]
10. Arif, M. Catalytic degradation of azo dyes by bimetallic nanoparticles loaded in smart polymer microgels. *RSC Adv.* **2023**, *13*, 3008–3019. [CrossRef]
11. Selim, M.T.; Salem, S.S.; Mohamed, A.A.; El-Gamal, M.S.; Awad, M.F.; Fouda, A. Biological Treatment of Real Textile Effluent Using Aspergillus flavus and Fusarium oxysporium and Their Consortium along with the Evaluation of Their Phytotoxicity. *J. Fungi* **2021**, *7*, 193. [CrossRef]
12. Tan, X.; Acquah, I.; Liu, H.; Li, W.; Tan, S. A critical review on saline wastewater treatment by membrane bioreactor (MBR) from a microbial perspective. *Chemosphere* **2019**, *220*, 1150–1162. [CrossRef]
13. Castrogiovanni, F.; Borea, L.; Corpuz, M.V.A.; Buonerba, A.; Vigliotta, G.; Ballesteros, F.J.; Hasan, S.W.; Belgiorno, V.; Naddeo, V. Innovative encapsulated self-forming dynamic bio-membrane bioreactor (ESFDMBR) for efficient wastewater treatment and fouling control. *Sci. Total Environ.* **2022**, *805*, 150296. [CrossRef]
14. Zhang, J.; Xiao, K.; Liu, Z.; Gao, T.; Liang, S.; Huang, X. Large-Scale Membrane Bioreactors for Industrial Wastewater Treatment in China: Technical and Economic Features, Driving Forces, and Perspectives. *Engineering* **2021**, *7*, 868–880. [CrossRef]
15. Deng, L.; Guo, W.; Ngo, H.H.; Zhang, X.; Chen, C.; Chen, Z.; Cheng, D.; Ni, S.-Q.; Wang, Q. Recent advances in attached growth membrane bioreactor systems for wastewater treatment. *Sci. Total Environ.* **2022**, *808*, 152123. [CrossRef]
16. Rondon, H.; El-Cheikh, W.; Boluarte, I.A.R.; Chang, C.-Y.; Bagshaw, S.; Farago, L.; Jegatheesan, V.; Shu, L. Application of enhanced membrane bioreactor (eMBR) to treat dye wastewater. *Bioresour. Technol.* **2015**, *183*, 78–85. [CrossRef]
17. Ravadelli, M.; da Costa, R.E.; Lobo-Recio, M.A.; Akaboci, T.R.V.; Bassin, J.P.; Lapolli, F.R.; Belli, T.J. Anoxic/oxic membrane bioreactor assisted by electrocoagulation for the treatment of azo-dye containing wastewater. *J. Environ. Chem. Eng.* **2021**, *9*, 105286. [CrossRef]
18. El-Kammah, M.; Elkhatib, E.; Gouveia, S.; Cameselle, C.; Aboukila, E. Cost-effective ecofriendly nanoparticles for rapid and efficient indigo carmine dye removal from wastewater: Adsorption equilibrium, kinetics and mechanism. *Environ. Technol. Innov.* **2022**, *28*, 102595. [CrossRef]
19. Nada, A.A.; Bekheet, M.F.; Roualdes, S.; Gurlo, A.; Ayral, A. Functionalization of MCM-41 with titanium oxynitride deposited via PECVD for enhanced removal of methylene blue. *J. Mol. Liq.* **2019**, *274*, 505–515. [CrossRef]
20. Artifon, W.; Cesca, K.; de Andrade, C.J.; Ulson de Souza, A.A.; de Oliveira, D. Dyestuffs from textile industry wastewaters: Trends and gaps in the use of bioflocculants. *Process Biochem.* **2021**, *111*, 181–190. [CrossRef]
21. Liu, Q. Pollution and Treatment of Dye Waste-Water. *IOP Conf. Ser. Earth Environ. Sci.* **2020**, *514*, 052001. [CrossRef]
22. Saba, B.; Kjellerup, B.V.; Christy, A.D. Eco-friendly bio-electro-degradation of textile dyes wastewater. *Bioresour. Technol. Rep.* **2021**, *15*, 100734. [CrossRef]
23. Shabir, G.; Arif, M.; Saeed, A.; Hussain, G. Synthesis and Optical Study of Sensitive and Selective Calix[4] Based Cu2+ Ion Detection Probes. *Russ. J. Gen. Chem.* **2019**, *89*, 813–818. [CrossRef]
24. Liu, Y.; Li, C.; Bao, J.; Wang, X.; Yu, W.; Shao, L. Degradation of Azo Dyes with Different Functional Groups in Simulated Wastewater by Electrocoagulation. *Water* **2022**, *14*, 123. [CrossRef]
25. Salem, S.; Fouda, A.; Mohamed, A.; El-Gamal, M.; Talat, M. Biological decolorization of azo dyes from textile wastewater effluent by Aspergillus niger. *Egypt. J. Chem.* **2019**, *62*, 1799–1813. [CrossRef]
26. Benkhaya, S.; El Harfi, S.; El Harfi, A. Classifications, properties and applications of textile dyes: A review. *Appl. J. Environ. Eng. Sci.* **2017**, *3*, 311–320.

27. Tajiki, A.; Abdouss, M. Synthesis and Characterization of Graphene Oxide Nano-sheets for Effective Removal of Copper Phthalocyanine from Aqueous Media. *Iran J. Chem. Chem. Eng.* **2017**, *36*, 1–9.
28. Lipatova, I.M.; Makarova, L.I.; Yusova, A.A. Adsorption removal of anionic dyes from aqueous solutions by chitosan nanoparticles deposited on the fibrous carrier. *Chemosphere* **2018**, *212*, 1155–1162. [CrossRef]
29. El Aggadi, S.; El Abbassi, Z.; El Hourch, A. Color removal from dye-containing aqueous solutions by electrooxidation. *Desalin. Water Treat.* **2021**, *215*, 232–236. [CrossRef]
30. Silva, M.C.; Corrêa, A.D.; Amorim, M.T.S.P.; Parpot, P.; Torres, J.A.; Chagas, P.M.B. Decolorization of the phthalocyanine dye reactive blue 21 by turnip peroxidase and assessment of its oxidation products. *J. Mol. Catal. B Enzym.* **2012**, *77*, 9–14. [CrossRef]
31. Beyhill, M.I.; Matthews, R.D.; Pavlostathis, S.G. Decolorization of a reactive copper-phthalocyanine dye under methanogenic conditions. *Water Sci. Technol.* **2001**, *43*, 333–340. [CrossRef]
32. Apostol, L.C.; Pereira, L.; Pereira, R.; Gavrilescu, M.; Alves, M.M. Biological decolorization of xanthene dyes by anaerobic granular biomass. *Biodegradation* **2012**, *23*, 725–737. [CrossRef]
33. Kiernan, J. Classification and naming of dyes, stains and fluorochromes. *Biotech. Histochem.* **2001**, *76*, 261–278. [CrossRef]
34. Niu, P.; Liang, X.; Lu, X.; Wang, S.; Li, Y.; Wang, L.; Guo, Y. Preparation of magnetic carbonized polyaniline nanotube and its adsorption behaviors of xanthene colorants in beverage and fish samples. *J. Chromatogr. A* **2019**, *1605*, 460369. [CrossRef]
35. Ikeno, T.; Nagano, T.; Hanaoka, K. Silicon-substituted Xanthene Dyes and Their Unique Photophysical Properties for Fluorescent Probes. *Chem. Asian J.* **2017**, *12*, 1435–1446. [CrossRef]
36. Kent, J.A. *Kent and Riegel's Handbook of Industrial Chemistry and Biotechnology*; Kent, J.A., Ed.; Springer: Boston, MA, USA, 2007; ISBN 978-0-387-27842-1.
37. dos Santos, G.C.; Oliveira, E.F.; Lavarda, F.C.; da Silva-Filho, L.C. Designing new quinoline-based organic photosensitizers for dye-sensitized solar cells (DSSC): A theoretical investigation. *J. Mol. Model.* **2019**, *25*, 75. [CrossRef]
38. Gupta, V.K.; Jain, R.; Agarwal, S.; Nayak, A.; Shrivastava, M. Photodegradation of hazardous dye quinoline yellow catalyzed by TiO2. *J. Colloid Interface Sci.* **2012**, *366*, 135–140. [CrossRef]
39. Wahyuningsih, S.; Ramelan, A.H.; Wardani, D.K.; Aini, F.N.; Sari, P.L.; Tamtama, B.P.N.; Kristiawan, Y.R. Indigo Dye Derived from Indigofera Tinctoria as Natural Food Colorant. *IOP Conf. Ser. Mater. Sci. Eng.* **2017**, *193*, 012048. [CrossRef]
40. Balan, D.S.L.; Monteiro, R.T.R. Decolorization of textile indigo dye by ligninolytic fungi. *J. Biotechnol.* **2001**, *89*, 141–145. [CrossRef]
41. Shaikh, M.; Swamy, Y.M.; Pal, H. Supramolecular host–guest interaction of acridine dye with cyclodextrin macrocycles: Photophysical, pKa shift and quenching study. *J. Photochem. Photobiol. A Chem.* **2013**, *258*, 41–50. [CrossRef]
42. Liu, S.P.; Chen, S.; Liu, Z.F.; Hu, X.L.; Li, T.S. Resonance Rayleigh scattering spectra of interaction of sodium carboxymethylcellulose with cationic acridine dyes and their analytical applications. *Anal. Chim. Acta* **2005**, *535*, 169–175. [CrossRef]
43. Yang, J.; Li, C.; Yang, Y.; Gu, J.; Bao, Q.; Lu, J.; Su, L.; Yang, L. Efficiency and mechanism of acridine orange removal by citric-acid-crosslinked β-cyclodextrin. *Mater. Lett.* **2022**, *312*, 131688. [CrossRef]
44. Devadiga, D.; Selvakumar, M.; Devadiga, D.; Paramasivam, S.; Ahipa, T.N.; Shetty, P.; Kumar, S.S. Organic sensitizer with azine π-conjugated architecture as co-sensitizer and polymer-based electrolyte for efficient dye-sensitized solar cell. *Surf. Interfaces* **2022**, *33*, 102236. [CrossRef]
45. Acar, E.T. An experimental and theoretical investigation of cationic azine dye adsorption on natural sepiolite in single and multi-component systems. *Chem. Eng. Res. Des.* **2022**, *187*, 507–515. [CrossRef]
46. Fanchiang, J.-M.; Tseng, D.-H. Degradation of anthraquinone dye C.I. Reactive Blue 19 in aqueous solution by ozonation. *Chemosphere* **2009**, *77*, 214–221. [CrossRef]
47. Deng, D.; Guo, J.; Zeng, G.; Sun, G. Decolorization of anthraquinone, triphenylmethane and azo dyes by a new isolated Bacillus cereus strain DC11. *Int. Biodeterior. Biodegrad.* **2008**, *62*, 263–269. [CrossRef]
48. Li, X.; Tang, S.; Yuan, D.; Tang, J.; Zhang, C.; Li, N.; Rao, Y. Improved degradation of anthraquinone dye by electrochemical activation of PDS. *Ecotoxicol. Environ. Saf.* **2019**, *177*, 77–85. [CrossRef]
49. Ogugbue, C.J.; Sawidis, T. Bioremediation and Detoxification of Synthetic Wastewater Containing Triarylmethane Dyes by Aeromonas hydrophila Isolated from Industrial Effluent. *Biotechnol. Res. Int.* **2011**, *2011*, 967925. [CrossRef]
50. Jeyaram, S. Intermolecular charge transfer in donor–acceptor substituted triarylmethane dye for NLO and optical limiting applications. *J. Mater. Sci. Mater. Electron.* **2021**, *32*, 9368–9376. [CrossRef]
51. Sakti, S.C.W.; Laily, R.N.; Aliyah, S.; Indrasari, N.; Fahmi, M.Z.; Lee, H.V.; Akemoto, Y.; Tanaka, S. Re-collectable and recyclable epichlorohydrin-crosslinked humic acid with spinel cobalt ferrite core for simple magnetic removal of cationic triarylmethane dyes in polluted water. *J. Environ. Chem. Eng.* **2020**, *8*, 104004. [CrossRef]
52. Pagalan Jr, E.; Sebron, M.; Gomez, S.; Salva, S.J.; Ampusta, R.; Macarayo, A.J.; Joyno, C.; Ido, A.; Arazo, R. Activated carbon from spent coffee grounds as an adsorbent for treatment of water contaminated by aniline yellow dye. *Ind. Crops Prod.* **2020**, *145*, 111953. [CrossRef]
53. Won, S.W.; Choi, S.B.; Yun, Y.-S. Performance and mechanism in binding of Reactive Orange 16 to various types of sludge. *Biochem. Eng. J.* **2006**, *28*, 208–214. [CrossRef]
54. Daneshvar, N.; Ashassi-Sorkhabi, H.; Tizpar, A. Decolorization of orange II by electrocoagulation method. *Sep. Purif. Technol.* **2003**, *31*, 153–162. [CrossRef]

55. Wong, Y.C.; Szeto, Y.S.; Cheung, W.H.; McKay, G. Adsorption of acid dyes on chitosan—Equilibrium isotherm analyses. *Process Biochem.* **2004**, *39*, 695–704. [CrossRef]
56. Fu, Y.; Viraraghavan, T. Removal of Congo Red from an aqueous solution by fungus Aspergillus niger. *Adv. Environ. Res.* **2002**, *7*, 239–247. [CrossRef]
57. PubChem Sudan IV. Available online: https://pubchem.ncbi.nlm.nih.gov/compound/62330 (accessed on 9 March 2023).
58. Singh, G.; Kumar, V.; Dwivedi, S.K. Comparative Investigation of Congo Red and Direct Blue-1 Adsorption on Mycosynthesized Iron Nanoparticle. *J. Clust. Sci.* **2022**, *33*, 1889–1905. [CrossRef]
59. Beluci, N.d.C.L.; Mateus, G.A.P.; Miyashiro, C.S.; Homem, N.C.; Gomes, R.G.; Fagundes-Klen, M.R.; Bergamasco, R.; Vieira, A.M.S. Hybrid treatment of coagulation/flocculation process followed by ultrafiltration in TIO2-modified membranes to improve the removal of reactive black 5 dye. *Sci. Total Environ.* **2019**, *664*, 222–229. [CrossRef]
60. Zhao, X.; Zhou, S.; Chen, M.; Wu, L. Effective encapsulation of Sudan black B with polystyrene using miniemulsion polymerization. *Colloid Polym. Sci.* **2009**, *287*, 969–977. [CrossRef]
61. Bulut, Y.; Gözübenli, N.; Aydın, H. Equilibrium and kinetics studies for adsorption of direct blue 71 from aqueous solution by wheat shells. *J. Hazard. Mater.* **2007**, *144*, 300–306. [CrossRef]
62. Alexandre, J.I.d.S.; Santos Neto, S.M.d.; Coutinho, A.P.; Melo, T.D.A.T.d.; Gonçalves, E.A.P.; Gondim, M.V.S.; Antonino, A.C.D.; Rabelo, A.E.C.d.G.d.C.; Oliveira, A.L.d. Sorption of the Direct Black 22 dye in alluvial soil. *Ambient. Agua-An Interdiscip. J. Appl. Sci.* **2020**, *15*, 1. [CrossRef]
63. PubChem Reactive Blue 21. Available online: https://pubchem.ncbi.nlm.nih.gov/compound/Reactive-Blue-21 (accessed on 9 March 2023).
64. Lee, Y.H.; Matthews, R.D.; Pavlostathis, S.G. Biological Decolorization of Reactive Anthraquinone and Phthalocyanine Dyes Under Various Oxidation-Reduction Conditions. *Water Environ. Res.* **2006**, *78*, 156–169. [CrossRef] [PubMed]
65. Imam, S.S.; Babamale, H.F. A Short Review on the Removal of Rhodamine B Dye Using Agricultural Waste-Based Adsorbents. *Asian J. Chem. Sci.* **2020**, *7*, 25–37. [CrossRef]
66. Walthall, W.; Stark, J. The acute and chronic toxicity of two xanthene dyes, fluorescein sodium salt and phloxine B, to Daphnia pulex. *Environ. Pollut.* **1999**, *104*, 207–215. [CrossRef]
67. Rashtbari, Y.; Afshin, S.; Hamzezadeh, A.; Gholizadeh, A.; Ansari, F.J.; Poureshgh, Y.; Fazlzadeh, M. Green synthesis of zinc oxide nanoparticles loaded on activated carbon prepared from walnut peel extract for the removal of Eosin Y and Erythrosine B dyes from aqueous solution: Experimental approaches, kinetics models, and thermodynamic studies. *Environ. Sci. Pollut. Res.* **2022**, *29*, 5194–5206. [CrossRef]
68. Bhatt, D.R.; Maheria, K.C.; Parikh, J.K. Highly efficient micellar extraction of toxic picric acid into novel ionic liquid: Effect of parameters, solubilization isotherm, evaluation of thermodynamics and design parameters. *J. Hazard. Mater.* **2015**, *300*, 338–346. [CrossRef]
69. Jain, R.; Gupta, V.K.; Sikarwar, S. Adsorption and desorption studies on hazardous dye Naphthol Yellow S. *J. Hazard. Mater.* **2010**, *182*, 749–756. [CrossRef]
70. Li, J.T.; Bai, B.; Song, Y.L. Degradation of Acid orange 3 in aqueous solution by combination of Fly ash/H2O2 and ultrasound irradiation. *Indian J. Chem. Technol.* **2010**, *17*, 198–203.
71. Hashemian, S.; Sadeghi, B.; Mozafari, F.; Salehfar, H.; Salari, K. Adsorption of Disperse of Yellow 42 onto Bentonite and Organo-Modified Bentonite by Tetra Butyl Ammonium Iodide (B-TBAI). *Pol. J. Environ. Stud.* **2013**, *22*, 1363–1370.
72. PubChem C.I. Disperse Yellow 70. Available online: https://pubchem.ncbi.nlm.nih.gov/compound/135666422 (accessed on 9 March 2023).
73. PubChem Quinoline Yellow. Available online: https://pubchem.ncbi.nlm.nih.gov/compound/6731 (accessed on 9 March 2023).
74. Ramesh, T.N.; Kirana, D.V.; Ashwini, A.; Manasa, T.R. Calcium hydroxide as low cost adsorbent for the effective removal of indigo carmine dye in water. *J. Saudi Chem. Soc.* **2017**, *21*, 165–171. [CrossRef]
75. PubChem 3,6-Bis(dimethylamino)acridine Hydrochloride. Available online: https://pubchem.ncbi.nlm.nih.gov/compound/517204 (accessed on 9 March 2023).
76. Solanki, V.S.; Ameta, K.L.; Pare, B.; Jonnalagadda, S.B.; Gupta, P. Investigation of photocatalytic mineralisation of Acridine Yellow G dye by BaCrO4 in the presence of eco-friendly LEDs irradiation. *J. Indian Chem. Soc.* **2022**, *99*, 100340. [CrossRef]
77. Ahmad, A.; Rafatullah, M.; Sulaiman, O.; Ibrahim, M.H.; Hashim, R. Scavenging behaviour of meranti sawdust in the removal of methylene blue from aqueous solution. *J. Hazard. Mater.* **2009**, *170*, 357–365. [CrossRef]
78. PubChem Thionine. Available online: https://pubchem.ncbi.nlm.nih.gov/compound/65043 (accessed on 9 March 2023).
79. Ghosh, I.; Kar, S.; Chatterjee, T.; Bar, N.; Das, S.K. Adsorptive removal of Safranin-O dye from aqueous medium using coconut coir and its acid-treated forms: Adsorption study, scale-up design, MPR and GA-ANN modeling. *Sustain. Chem. Pharm.* **2021**, *19*, 100374. [CrossRef]
80. Daneshvar, E.; Sohrabi, M.S.; Kousha, M.; Bhatnagar, A.; Aliakbarian, B.; Converti, A.; Norrström, A.-C. Shrimp shell as an efficient bioadsorbent for Acid Blue 25 dye removal from aqueous solution. *J. Taiwan Inst. Chem. Eng.* **2014**, *45*, 2926–2934. [CrossRef]
81. PubChem Disperse Red 11. Available online: https://pubchem.ncbi.nlm.nih.gov/compound/17885 (accessed on 9 March 2023).
82. PubChem Reactive Blue 19. Available online: https://pubchem.ncbi.nlm.nih.gov/compound/17409 (accessed on 9 March 2023).

83. Janaki, V.; Vijayaraghavan, K.; Ramasamy, A.K.; Lee, K.-J.; Oh, B.-T.; Kamala-Kannan, S. Competitive adsorption of Reactive Orange 16 and Reactive Brilliant Blue R on polyaniline/bacterial extracellular polysaccharides composite—A novel eco-friendly polymer. *J. Hazard. Mater.* **2012**, *241–242*, 110–117. [CrossRef]
84. Huang, L.; Kong, J.; Wang, W.; Zhang, C.; Niu, S.; Gao, B. Study on Fe(III) and Mn(II) modified activated carbons derived from Zizania latifolia to removal basic fuchsin. *Desalination* **2012**, *286*, 268–276. [CrossRef]
85. Sartape, A.S.; Mandhare, A.M.; Jadhav, V.V.; Raut, P.D.; Anuse, M.A.; Kolekar, S.S. Removal of malachite green dye from aqueous solution with adsorption technique using Limonia acidissima (wood apple) shell as low cost adsorbent. *Arab. J. Chem.* **2017**, *10*, S3229–S3238. [CrossRef]
86. PubChem Gentian Violet. Available online: https://pubchem.ncbi.nlm.nih.gov/compound/11057 (accessed on 9 March 2023).
87. Shamsipur, M.; Rajabi, H.R. Study of photocatalytic activity of ZnS quantum dots as efficient nanoparticles for removal of methyl violet: Effect of ferric ion doping. *Spectrochim. Acta Part A Mol. Biomol. Spectrosc.* **2014**, *122*, 260–267. [CrossRef]
88. Gita, S.; Hussan, A.; Choudhury, T.G. Impact of Textile Dyes Waste on Aquatic Environments and its Treatment. *Environ. Ecol.* **2017**, *35*, 2349–2353.
89. Hernández-Zamora, M.; Martínez-Jerónimo, F.; Cristiani-Urbina, E.; Cañizares-Villanueva, R.O. Congo red dye affects survival and reproduction in the cladoceran Ceriodaphnia dubia. Effects of direct and dietary exposure. *Ecotoxicology* **2016**, *25*, 1832–1840. [CrossRef]
90. Krishna Moorthy, A.; Govindarajan Rathi, B.; Shukla, S.P.; Kumar, K.; Shree Bharti, V. Acute toxicity of textile dye Methylene blue on growth and metabolism of selected freshwater microalgae. *Environ. Toxicol. Pharmacol.* **2021**, *82*, 103552. [CrossRef]
91. Gita, S.; Shukla, S.P.; Deshmukhe, G.; Choudhury, T.G.; Saharan, N.; Singh, A.K. Toxicity Evaluation of Six Textile Dyes on Growth, Metabolism and Elemental Composition (C, H, N, S) of Microalgae Spirulina platensis: The Environmental Consequences. *Bull. Environ. Contam. Toxicol.* **2021**, *106*, 302–309. [CrossRef] [PubMed]
92. Marimuthu, S.; Antonisamy, A.J.; Malayandi, S.; Rajendran, K.; Tsai, P.-C.; Pugazhendhi, A.; Ponnusamy, V.K. Silver nanoparticles in dye effluent treatment: A review on synthesis, treatment methods, mechanisms, photocatalytic degradation, toxic effects and mitigation of toxicity. *J. Photochem. Photobiol. B Biol.* **2020**, *205*, 111823. [CrossRef] [PubMed]
93. Jiang, X.; Kopp-Schneider, A. Summarizing EC50 estimates from multiple dose-response experiments: A comparison of a meta-analysis strategy to a mixed-effects model approach. *Biom. J.* **2014**, *56*, 493–512. [CrossRef] [PubMed]
94. Skjolding, L.M.; Jørgensen, L.G.; Dyhr, K.S.; Köppl, C.J.; McKnight, U.S.; Bauer-Gottwein, P.; Mayer, P.; Bjerg, P.L.; Baun, A. Assessing the aquatic toxicity and environmental safety of tracer compounds Rhodamine B and Rhodamine WT. *Water Res.* **2021**, *197*, 117109. [CrossRef]
95. Novotný, Č.; Dias, N.; Kapanen, A.; Malachová, K.; Vándrovcová, M.; Itävaara, M.; Lima, N. Comparative use of bacterial, algal and protozoan tests to study toxicity of azo- and anthraquinone dyes. *Chemosphere* **2006**, *63*, 1436–1442. [CrossRef]
96. Gita, S.; Shukla, S.P.; Prakash, C.; Saharan, N.; Deshmukhe, G. Evaluation of Toxicity of a Textile Dye (Optilan Red) towards a Green Microalga Chlorella vulgaris. *Int. J. Curr. Microbiol. Appl. Sci.* **2018**, *7*, 3346–3355. [CrossRef]
97. Vinitnantharat, S.; Chartthe, W.; Pinisakul, A. Toxicity of reactive red 141 and basic red 14 to algae and waterfleas. *Water Sci. Technol.* **2008**, *58*, 1193–1198. [CrossRef]
98. Srivastava, S.; Sinha, R.; Roy, D. Toxicological effects of malachite green. *Aquat. Toxicol.* **2004**, *66*, 319–329. [CrossRef]
99. Köktürk, M. In vivo toxicity assessment of Remazol Gelb–GR (RG-GR) textile dye in zebrafish embryos/larvae (Danio rerio): Teratogenic effects, biochemical changes, immunohistochemical changes. *Sci. Total Environ.* **2022**, *852*, 158473. [CrossRef]
100. Hussain, B.; Sajad, M.; Usman, H.; Al-Ghanim, K.A.; Riaz, M.N.; Berenjian, A.; Mahboob, S.; Show, P.L. Assessment of hepatotoxicity and nephrotoxicity in Cirrhinus mrigala induced by trypan blue—An azo dye. *Environ. Res.* **2022**, *215*, 114120. [CrossRef]
101. Parrott, J.L.; Bartlett, A.J.; Balakrishnan, V.K. Chronic toxicity of azo and anthracenedione dyes to embryo-larval fathead minnow. *Environ. Pollut.* **2016**, *210*, 40–47. [CrossRef]
102. Elmoutez, S.; Abushaban, A.; Necibi, M.C.; Sillanpää, M.; Liu, J.; Dhiba, D.; Chehbouni, A.; Taky, M. Design and operational aspects of anaerobic membrane bioreactor for efficient wastewater treatment and biogas production. *Environ. Chall.* **2023**, *10*, 100671. [CrossRef]
103. Wijaya, J.; Oh, S. Machine learning reveals the complex ecological interplay of microbiome in a full-scale membrane bioreactor wastewater treatment plant. *Environ. Res.* **2023**, *222*, 115366. [CrossRef]
104. Lin, H.; Peng, W.; Zhang, M.; Chen, J.; Hong, H.; Zhang, Y. A review on anaerobic membrane bioreactors: Applications, membrane fouling and future perspectives. *Desalination* **2013**, *314*, 169–188. [CrossRef]
105. George, J.; Kumar, V.V. Designing a novel poly (methyl vinyl ether maleic anhydride) based polymeric membrane with enhanced antifouling performance for removal of pentachlorophenol from aqueous solution. *Environ. Res.* **2023**, *223*, 115404. [CrossRef]
106. Baig, U.; Waheed, A. An efficient and simple strategy for fabricating a polypyrrole decorated ceramic-polymeric porous membrane for purification of a variety of oily wastewater streams. *Environ. Res.* **2023**, *219*, 114959. [CrossRef]
107. Huang, J.; Chen, H.; Yang, J.; Zhou, T.; Zhang, H. Effects of particle size on microstructure and mechanical strength of a fly ash based ceramic membrane. *Ceram. Int.* **2023**, *in press*. [CrossRef]
108. Zhao, M.; Liu, Y.; Zhang, J.; Jiang, H.; Chen, R. Janus ceramic membranes with asymmetric wettability for high-efficient microbubble aeration. *J. Memb. Sci.* **2023**, *671*, 121418. [CrossRef]

109. Aalami-Aleagha, M.E.; Madaeni, S.S.; Daraei, P. A New Application of Thermal Spray in Preparation of Metallic Membrane for Concentration of Glucose Solution. *J. Therm. Spray Technol.* **2009**, *18*, 519–524. [CrossRef]
110. Yurtsever, A.; Sahinkaya, E.; Aktaş, Ö.; Uçar, D.; Çınar, Ö.; Wang, Z. Performances of anaerobic and aerobic membrane bioreactors for the treatment of synthetic textile wastewater. *Bioresour. Technol.* **2015**, *192*, 564–573. [CrossRef]
111. Batstone, D.J.; Virdis, B. The role of anaerobic digestion in the emerging energy economy. *Curr. Opin. Biotechnol.* **2014**, *27*, 142–149. [CrossRef] [PubMed]
112. Ji, J.; Kakade, A.; Yu, Z.; Khan, A.; Liu, P.; Li, X. Anaerobic membrane bioreactors for treatment of emerging contaminants: A review. *J. Environ. Manag.* **2020**, *270*, 110913. [CrossRef] [PubMed]
113. Maaz, M.; Yasin, M.; Aslam, M.; Kumar, G.; Atabani, A.E.; Idrees, M.; Anjum, F.; Jamil, F.; Ahmad, R.; Khan, A.L.; et al. Anaerobic membrane bioreactors for wastewater treatment: Novel configurations, fouling control and energy considerations. *Bioresour. Technol.* **2019**, *283*, 358–372. [CrossRef] [PubMed]
114. Li, J.; Jiang, J.; Li, J.; He, C.; Luo, Y.; Wei, L. Anaerobic membrane bioreactors for wastewater treatment: Mechanisms, fouling control, novel configurations, and future perspectives. *Environ. Eng. Res.* **2022**, *28*, 210575. [CrossRef]
115. Fairley-Wax, T.; Raskin, L.; Skerlos, S.J. Recirculating Anaerobic Dynamic Membrane Bioreactor Treatment of Municipal Wastewater. *ACS ES&T Eng.* **2022**, *2*, 842–852. [CrossRef]
116. Zhang, H.; Wang, H.; Jie, M.; Zhang, K.; Qian, Y.; Ma, J. Performance and microbial communities of different biofilm membrane bioreactors with pre-anoxic tanks treating mariculture wastewater. *Bioresour. Technol.* **2020**, *295*, 122302. [CrossRef]
117. Raj Deena, S.; Kumar, G.; Vickram, A.S.; Rani Singhania, R.; Dong, C.; Rohini, K.; Anbarasu, K.; Thanigaivel, S.; Ponnusamy, V.K. Efficiency of various biofilm carriers and microbial interactions with substrate in moving bed-biofilm reactor for environmental wastewater treatment. *Bioresour. Technol.* **2022**, *359*, 127421. [CrossRef]
118. Zhao, K.; Su, F.; Gu, K.; Qi, J.; Liu, R.; Hu, C. Antifouling potential and microbial characterization of an electrochemical anaerobic membrane bioreactor utilizing membrane cathode and iron anode. *Bioresour. Technol.* **2021**, *334*, 125230. [CrossRef]
119. Yao, M.; Woo, Y.C.; Ren, J.; Tijing, L.D.; Choi, J.-S.; Kim, S.-H.; Shon, H.K. Volatile fatty acids and biogas recovery using thermophilic anaerobic membrane distillation bioreactor for wastewater reclamation. *J. Environ. Manag.* **2019**, *231*, 833–842. [CrossRef]
120. Moideen, S.N.F.; Krishnan, S.; Li, Y.-Y.; Hassim, M.H.; Kamyab, H.; Nasrullah, M.; Din, M.F.M.; Halim, K.A.; Chaiprapat, S. Performance evaluation and energy potential analysis of anaerobic membrane bioreactor (AnMBR) in the treatment of simulated milk wastewater. *Chemosphere* **2023**, *317*, 137923. [CrossRef]
121. Chen, H.; Yuan, J.; Yang, E.; Yang, T.; Shi, L.; Liu, Z.; Yu, H.; Cao, J.; Kong, Z.; Zhou, Q.; et al. Swine wastewater treatment using combined up-flow anaerobic sludge blanket and anaerobic membrane bioreactor: Performance and microbial community diversity. *Bioresour. Technol.* **2023**, *373*, 128606. [CrossRef]
122. Ramadan, L.; Deeb, R.; Sawaya, C.; El Khoury, C.; Wazne, M.; Harb, M. Anaerobic membrane bioreactor-based treatment of poultry slaughterhouse wastewater: Microbial community adaptation and antibiotic resistance gene profiles. *Biochem. Eng. J.* **2023**, *192*, 108847. [CrossRef]
123. Li, N.; He, L.; Lu, Y.-Z.; Zeng, R.J.; Sheng, G.-P. Robust performance of a novel anaerobic biofilm membrane bioreactor with mesh filter and carbon fiber (ABMBR) for low to high strength wastewater treatment. *Chem. Eng. J.* **2017**, *313*, 56–64. [CrossRef]
124. Keerthi; Suganthi, V.; Mahalakshmi, M.; Balasubramanian, N. Development of hybrid membrane bioreactor for tannery effluent treatment. *Desalination* **2013**, *309*, 231–236. [CrossRef]
125. Yurtsever, A.; Basaran, E.; Ucar, D.; Sahinkaya, E. Self-forming dynamic membrane bioreactor for textile industry wastewater treatment. *Sci. Total Environ.* **2021**, *751*, 141572. [CrossRef]
126. Sari Erkan, H.; Çağlak, A.; Soysaloglu, A.; Takatas, B.; Onkal Engin, G. Performance evaluation of conventional membrane bioreactor and moving bed membrane bioreactor for synthetic textile wastewater treatment. *J. Water Process Eng.* **2020**, *38*, 101631. [CrossRef]
127. Yurtsever, A.; Basaran, E.; Ucar, D. Process optimization and filtration performance of an anaerobic dynamic membrane bioreactor treating textile wastewaters. *J. Environ. Manag.* **2020**, *273*, 111114. [CrossRef]
128. Katuri, K.P.; Werner, C.M.; Jimenez-Sandoval, R.J.; Chen, W.; Jeon, S.; Logan, B.E.; Lai, Z.; Amy, G.L.; Saikaly, P.E. A Novel Anaerobic Electrochemical Membrane Bioreactor (AnEMBR) with Conductive Hollow-fiber Membrane for Treatment of Low-Organic Strength Solutions. *Environ. Sci. Technol.* **2014**, *48*, 12833–12841. [CrossRef]
129. Azimi, B.; Abdollahzadeh-Sharghi, E.; Bonakdarpour, B. Anaerobic-aerobic processes for the treatment of textile dyeing wastewater containing three commercial reactive azo dyes: Effect of number of stages and bioreactor type. *Chin. J. Chem. Eng.* **2021**, *39*, 228–239. [CrossRef]
130. Manzoor, K.; Khan, S.J.; Yasmeen, M.; Jamal, Y.; Arshad, M. Assessment of anaerobic membrane distillation bioreactor hybrid system at mesophilic and thermophilic temperatures treating textile wastewater. *J. Water Process Eng.* **2022**, *46*, 102603. [CrossRef]
131. Manzoor, K.; Khan, S.J.; Khan, A.; Abbasi, H.; Zaman, W.Q. Woven-fiber microfiltration coupled with anaerobic forward osmosis membrane bioreactor treating textile wastewater: Use of fertilizer draw solutes for direct fertigation. *Biochem. Eng. J.* **2022**, *181*, 108385. [CrossRef]

132. Bai, Y.-N.; Wang, X.-N.; Zhang, F.; Wu, J.; Zhang, W.; Lu, Y.-Z.; Fu, L.; Lau, T.-C.; Zeng, R.J. High-rate anaerobic decolorization of methyl orange from synthetic azo dye wastewater in a methane-based hollow fiber membrane bioreactor. *J. Hazard. Mater.* **2020**, *388*, 121753. [CrossRef] [PubMed]
133. Liu, J.; Xiong, J.; Tian, C.; Gao, B.; Wang, L.; Jia, X. The degradation of methyl orange and membrane fouling behavior in anaerobic baffled membrane bioreactor. *Chem. Eng. J.* **2018**, *338*, 719–725. [CrossRef]
134. Castro, F.D.; Bassin, J.P.; Alves, T.L.M.; Sant'Anna, G.L.; Dezotti, M. Reactive Orange 16 dye degradation in anaerobic and aerobic MBBR coupled with ozonation: Addressing pathways and performance. *Int. J. Environ. Sci. Technol.* **2021**, *18*, 1991–2010. [CrossRef]
135. Choerudin, C.; Arrahmah, F.I.; Daniel, J.K.; Watari, T.; Yamaguchi, T.; Setiadi, T. Evaluation of combined anaerobic membrane bioreactor and downflow hanging sponge reactor for treatment of synthetic textile wastewater. *J. Environ. Chem. Eng.* **2021**, *9*, 105276. [CrossRef]
136. Zhang, W.; Liu, F.; Wang, D.; Jin, Y. Impact of reactor configuration on treatment performance and microbial diversity in treating high-strength dyeing wastewater: Anaerobic flat-sheet ceramic membrane bioreactor versus upflow anaerobic sludge blanket reactor. *Bioresour. Technol.* **2018**, *269*, 269–275. [CrossRef]
137. Sahinkaya, E.; Yurtsever, A.; Çınar, Ö. Treatment of textile industry wastewater using dynamic membrane bioreactor: Impact of intermittent aeration on process performance. *Sep. Purif. Technol.* **2017**, *174*, 445–454. [CrossRef]
138. Baêta, B.E.L.; Lima, D.R.S.; Silva, S.Q.; Aquino, S.F. Influence of the applied organic load (OLR) on textile wastewater treatment using submerged anaerobic membrane bioreactors (SAMBR) in the presence of redox mediator and powdered activated carbon (PAC). *Braz. J. Chem. Eng.* **2016**, *33*, 817–825. [CrossRef]
139. Jin, Y.; Wang, D.; Zhang, W. Newly Designed Hydrolysis Acidification Flat-Sheet Ceramic Membrane Bioreactor for Treating High-Strength Dyeing Wastewater. *Int. J. Environ. Res. Public Health* **2019**, *16*, 777. [CrossRef]
140. Jegatheesan, V.; Pramanik, B.K.; Chen, J.; Navaratna, D.; Chang, C.-Y.; Shu, L. Treatment of textile wastewater with membrane bioreactor: A critical review. *Bioresour. Technol.* **2016**, *204*, 202–212. [CrossRef]
141. Mutamim, N.S.A.; Noor, Z.Z.; Hassan, M.A.A.; Olsson, G. Application of membrane bioreactor technology in treating high strength industrial wastewater: A performance review. *Desalination* **2012**, *305*, 1–11. [CrossRef]
142. Januário, E.F.D.; Vidovix, T.B.; Beluci, N.d.C.L.; Paixão, R.M.; Silva, L.H.B.R.d.; Homem, N.C.; Bergamasco, R.; Vieira, A.M.S. Advanced graphene oxide-based membranes as a potential alternative for dyes removal: A review. *Sci. Total Environ.* **2021**, *789*, 147957. [CrossRef]
143. Joshi, R.K.; Carbone, P.; Wang, F.C.; Kravets, V.G.; Su, Y.; Grigorieva, I.V.; Wu, H.A.; Geim, A.K.; Nair, R.R. Precise and Ultrafast Molecular Sieving Through Graphene Oxide Membranes. *Science* **2014**, *343*, 752–754. [CrossRef]
144. Diogo Januário, E.F.; de Camargo Lima Beluci, N.; Vidovix, T.B.; Vieira, M.F.; Bergamasco, R.; Salcedo Vieira, A.M. Functionalization of membrane surface by layer-by-layer self-assembly method for dyes removal. *Process Saf. Environ. Prot.* **2020**, *134*, 140–148. [CrossRef]
145. Rashidi, H.R.; Sulaiman, N.M.N.; Hashim, N.A.; Hassan, C.R.C.; Ramli, M.R. Synthetic reactive dye wastewater treatment by using nano-membrane filtration. *Desalin. Water Treat.* **2015**, *55*, 86–95. [CrossRef]
146. Ding, J.; Pu, L.; Zou, D.; Cao, M.; Shan, C.; Zhang, Q.; Gao, G.; Pan, B. Removal of model dyes on charged UF membranes: Experiment and simulation. *Chemosphere* **2020**, *240*, 124940. [CrossRef]
147. Zhong, P.S.; Widjojo, N.; Chung, T.-S.; Weber, M.; Maletzko, C. Positively charged nanofiltration (NF) membranes via UV grafting on sulfonated polyphenylenesulfone (sPPSU) for effective removal of textile dyes from wastewater. *J. Memb. Sci.* **2012**, *417–418*, 52–60. [CrossRef]
148. Gnanasekaran, G.; Sudhakaran, M.S.P.; Kulmatova, D.; Han, J.; Arthanareeswaran, G.; Jwa, E.; Mok, Y.S. Efficient removal of anionic, cationic textile dyes and salt mixture using a novel CS/MIL-100 (Fe) based nanofiltration membrane. *Chemosphere* **2021**, *284*, 131244. [CrossRef]
149. Bromley-Challenor, K. Decolorization of an azo dye by unacclimated activated sludge under anaerobic conditions. *Water Res.* **2000**, *34*, 4410–4418. [CrossRef]
150. Türgay, O.; Ersöz, G.; Atalay, S.; Forss, J.; Welander, U. The treatment of azo dyes found in textile industry wastewater by anaerobic biological method and chemical oxidation. *Sep. Purif. Technol.* **2011**, *79*, 26–33. [CrossRef]
151. Khalili, Z.; Bonakdarpour, B. Statistical Optimization of Anaerobic Biological Processes for Dye Treatment. *CLEAN-Soil Air Water* **2010**, *38*, 942–950. [CrossRef]
152. Fang, F.; Cao, J.S.; Chen, L.; Chen, L.; Feng, Q.; Xu, H. Enhanced performance of dyeing wastewater reclamation by PAC addition in a membrane bioreactor. *J. Food Agric. Environ.* **2012**, *10*, 1138–1141.
153. Zhou, Z.; Tao, Y.; Zhang, S.; Xiao, Y.; Meng, F.; Stuckey, D.C. Size-dependent microbial diversity of sub-visible particles in a submerged anaerobic membrane bioreactor (SAnMBR): Implications for membrane fouling. *Water Res.* **2019**, *159*, 20–29. [CrossRef] [PubMed]
154. Niu, C.; Pan, Y.; Lu, X.; Wang, S.; Zhang, Z.; Zheng, C.; Tan, Y.; Zhen, G.; Zhao, Y.; Li, Y.-Y. Mesophilic anaerobic digestion of thermally hydrolyzed sludge in anaerobic membrane bioreactor: Long-term performance, microbial community dynamics and membrane fouling mitigation. *J. Memb. Sci.* **2020**, *612*, 118264. [CrossRef]
155. Liao, Y.; Wang, Y.; Ouyang, L.; Dong, Y.; Zhou, J.; Hu, Q.; Qiu, B. Conductive Polyaniline Enhanced Decolorization of Azo Dyes in Anaerobic Wastewater Treatment. *ES Food Agrofor.* **2021**, *6*, 35–42. [CrossRef]

156. Chaudhari, A.; Paul, D.; Thamke, V.; Bagade, A.; Bapat, V.A.; Kodam, K.M. Concurrent removal of reactive blue HERD dye and Cr(VI) by aerobic bacterial granules. *J. Clean. Prod.* **2022**, *367*, 133075. [CrossRef]
157. Yang, B.; Xu, H.; Yang, S.; Bi, S.; Li, F.; Shen, C.; Ma, C.; Tian, Q.; Liu, J.; Song, X.; et al. Treatment of industrial dyeing wastewater with a pilot-scale strengthened circulation anaerobic reactor. *Bioresour. Technol.* **2018**, *264*, 154–162. [CrossRef]
158. Chen, H.; Liu, Y.; Xu, X.; Sun, M.; Jiang, M.; Xue, G.; Li, X.; Liu, Z. How does iron facilitate the aerated biofilter for tertiary simultaneous nutrient and refractory organics removal from real dyeing wastewater? *Water Res.* **2019**, *148*, 344–358. [CrossRef]
159. Qiu, B.; Xu, X.; Dang, Y.; Wang, Q.; Sun, D.; Wei, S.; Guo, Z. Biotransformative removal of cationic Red X-GRL by anaerobic activated sludge. *RSC Adv.* **2015**, *5*, 25699–25707. [CrossRef]
160. Zhang, L. Molecular diversity of bacterial community of dye wastewater in an anaerobic sequencing batch reactor. *Afr. J. Microbiol. Res.* **2012**, *6*, 6444–6453. [CrossRef]
161. Dai, Q.; Zhang, S.; Liu, H.; Huang, J.; Li, L. Sulfide-mediated azo dye degradation and microbial community analysis in a single-chamber air cathode microbial fuel cell. *Bioelectrochemistry* **2020**, *131*, 107349. [CrossRef]
162. Kong, Z.; Li, L.; Xue, Y.; Yang, M.; Li, Y.-Y. Challenges and prospects for the anaerobic treatment of chemical-industrial organic wastewater: A review. *J. Clean. Prod.* **2019**, *231*, 913–927. [CrossRef]
163. Hamedi, H.; Ehteshami, M.; Mirbagheri, S.A.; Rasouli, S.A.; Zendehboudi, S. Current Status and Future Prospects of Membrane Bioreactors (MBRs) and Fouling Phenomena: A Systematic Review. *Can. J. Chem. Eng.* **2019**, *97*, 32–58. [CrossRef]
164. Huang, Z.; Ong, S.L.; Ng, H.Y. Submerged anaerobic membrane bioreactor for low-strength wastewater treatment: Effect of HRT and SRT on treatment performance and membrane fouling. *Water Res.* **2011**, *45*, 705–713. [CrossRef]
165. Nabi, M.; Liang, H.; Zhou, Q.; Cao, J.; Gao, D. In-situ membrane fouling control and performance improvement by adding materials in anaerobic membrane bioreactor: A review. *Sci. Total Environ.* **2023**, *865*, 161262. [CrossRef]
166. Gul, A.; Hruza, J.; Dvorak, L.; Yalcinkaya, F. Chemical Cleaning Process of Polymeric Nanofibrous Membranes. *Polymers* **2022**, *14*, 1102. [CrossRef]
167. Shahid, M.K.; Kashif, A.; Rout, P.R.; Aslam, M.; Fuwad, A.; Choi, Y.; Banu, J.R.; Park, J.H.; Kumar, G. A brief review of anaerobic membrane bioreactors emphasizing recent advancements, fouling issues and future perspectives. *J. Environ. Manag.* **2020**, *270*, 110909. [CrossRef]